International Journal of Greenhouse Gas Control 40 (2015) 221–237

Contents lists available at ScienceDirect

International Journal of Greenhouse Gas Control

journal homepage: www.elsevier.com/locate/ijggc

Capillary trapping for geologic carbon dioxide storage – From pore scale physics to field scale implications

Samuel Krevor[a,b,*], Martin J. Blunt[a,b], Sally M. Benson[c], Christopher H. Pentland[d], Catriona Reynolds[a,b], Ali Al-Menhali[a,b], Ben Niu[a,b]

[a] Department of Earth Science and Engineering, Imperial College London, London, UK
[b] Qatar Carbonates and Carbon Storage Research Centre, Imperial College London, London, UK
[c] Department of Energy Resources Engineering, Stanford University, Stanford, USA
[d] Petroleum Development Oman, Oman

ARTICLE INFO

Article history:
Received 5 January 2015
Received in revised form 4 April 2015
Accepted 7 April 2015
Available online 25 April 2015

Keywords:
Capillary trapping
Residual trapping
Multiphase flow
CO_2 sequestration

ABSTRACT

A significant amount of theoretical, numerical and observational work has been published focused on various aspects of capillary trapping in CO_2 storage since the IPCC Special Report on Carbon Dioxide Capture and Storage (2005). This research has placed capillary trapping in a central role in nearly every aspect of the geologic storage of CO_2. Capillary, or residual, trapping – where CO_2 is rendered immobile in the pore space as disconnected ganglia, surrounded by brine in a storage aquifer – is controlled by fluid and interfacial physics at the size scale of rock pores. These processes have been observed at the pore scale in situ using X-ray microtomography at reservoir conditions. A large database of conventional centimetre core scale observations for flow modelling are now available for a range of rock types and reservoir conditions. These along with the pore scale observations confirm that trapped saturations will be at least 10% and more typically 30% of the pore volume of the rock, stable against subsequent displacement by brine and characteristic of water-wet systems. Capillary trapping is pervasive over the extent of a migrating CO_2 plume and both theoretical and numerical investigations have demonstrated the first order impacts of capillary trapping on plume migration, immobilisation and CO_2 storage security. Engineering strategies to maximise capillary trapping have been proposed that make use of injection schemes that maximise sweep or enhance imbibition. National assessments of CO_2 storage capacity now incorporate modelling of residual trapping where it can account for up to 95% of the storage resource. Field scale observations of capillary trapping have confirmed the formation and stability of residually trapped CO_2 at masses up to 10,000 tons and over time scales of years. Significant outstanding uncertainties include the impact of heterogeneity on capillary immobilisation and capillary trapping in mixed-wet systems. Overall capillary trapping is well constrained by laboratory and field scale observations, effectively modelled in theoretical and numerical models and significantly enhances storage integrity, both increasing storage capacity and limiting the rate and extent of plume migration.

1. Introduction

The trapping of CO_2 by capillary forces in the pore space of rocks is a key process for maximising capacity and ensuring the integrity of CO_2 sequestration at industrial scales. When CO_2 is injected into a deep subsurface geologic formation it will displace the resident fluid, generally brine and in some cases hydrocarbons, and migrate in response to buoyancy and pressure gradients. As the reservoir brine imbibes back into the pore space pursuant to the migrating CO_2 plume, small isolated blobs of CO_2 will be trapped by capillary forces: this is known as capillary or residual trapping (Fig. 1). The isolated blobs are of the size scale of the pores of the rocks, tens to hundreds of micrometers, and the process is controlled by fluid physics and interfacial forces at the micron scale. Because the trapping, however, is pervasive over the hundreds of meters to hundreds of kilometres of the plume extent it plays a major role in plume migration, immobilisation, storage security and ultimately the capacity for storage resources to safely contain injected CO_2.

The importance of capillary trapping had already been identified in the IPCC Special Report on Carbon Dioxide Capture and Storage (IPCC, 2005). Both the extent and rate of trapping made it integral

* Corresponding author at: Department of Earth Science and Engineering, Imperial College London, London, UK. Tel.: +44 02075942701.
E-mail address: s.krevor@imperial.ac.uk (S. Krevor).

http://dx.doi.org/10.1016/j.ijggc.2015.04.006

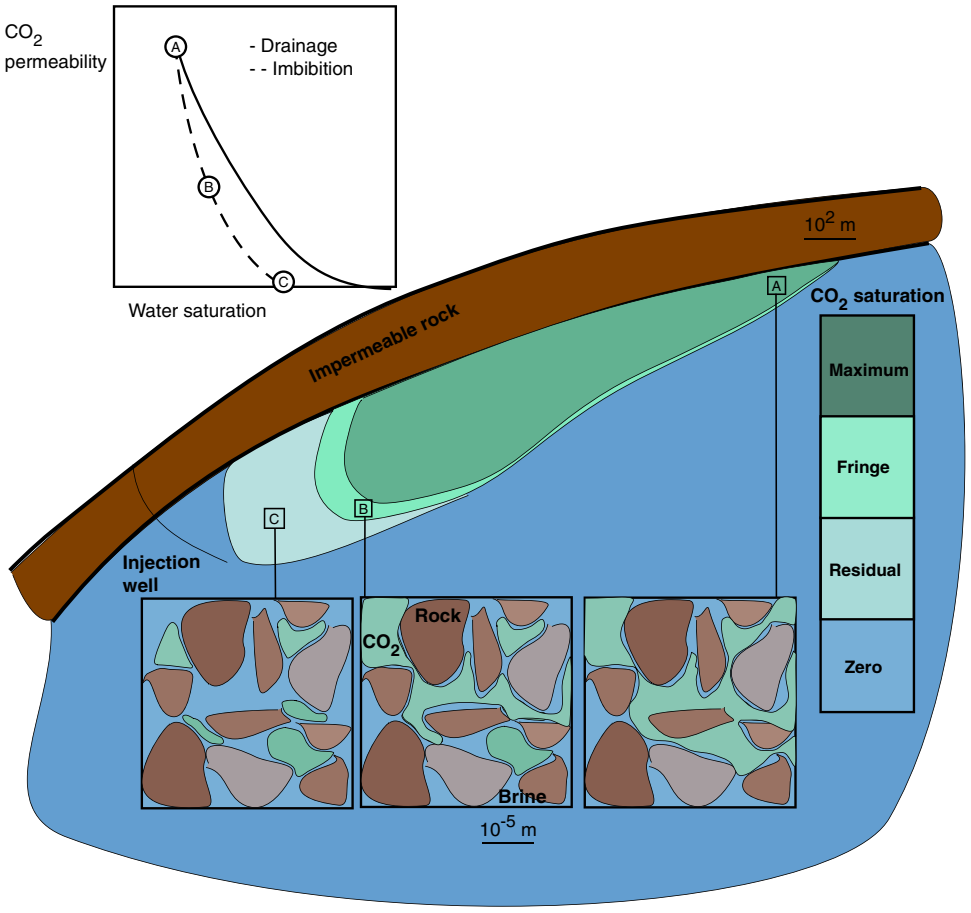

Fig. 1. A sketch of key processes governed by capillary trapping after CO_2 injection has ceased at a storage site. Plume migration is limited by the trapping as large fractions of the plume are immobilised. Capillary trapping is secure over long timescales and avoids buoyant stress on overlying cap rock layers. Trapping is also key to parameterising hysteresis in relative permeability functions – more trapping leads to greater disconnection of fluid ganglia as CO_2 saturation in the pore space decreases (movement from A towards C in the figure) and thus a larger decrease in permeability as a function of saturation.

to storage security relative to other trapping mechanisms (Fig. 2). At the time of the report, the importance of capillary trapping for CO_2 migration and immobilisation had been identified in a small number of numerical studies (King and Paterson, 2002; Doughty and Pruess, 2004), but no laboratory or field observations of the extent of trapping had been published, the pore scale interfacial properties had not been characterised and no methodology incorporated residual trapping in estimations of the storage capacity of individual sites or regions.

In this paper we review the body of work, most of which has been published in the ten years since the IPCC report, that has placed capillary trapping in a central role in nearly every aspect of the geological storage of CO_2. The recently developed tools of digital rock physics has allowed for unprecedented detail in understanding the pore scale physics of CO_2-brine systems. A sizeable and growing database of observations of the key constitutive relationship characterising capillary trapping at the centimetre scale of rock cores now exists for a range of rock types and reservoir conditions. The impact of capillary trapping on plume migration and immobilisation is now well understood from both theoretical and numerical investigations. Where CO_2 storage constitutes an ongoing component of greenhouse gas emissions abatement strategy, governmental agencies now incorporate modelling of residual trapping at field scales for estimations of the capacity of the regional storage resource. The existence and stability of residually trapped CO_2 in reservoir settings has been demonstrated by field scale injection experiments in Japan, the United States and Australia (Xue et al., 2006; Hovorka et al., 2006; Paterson et al., 2011). Combined,

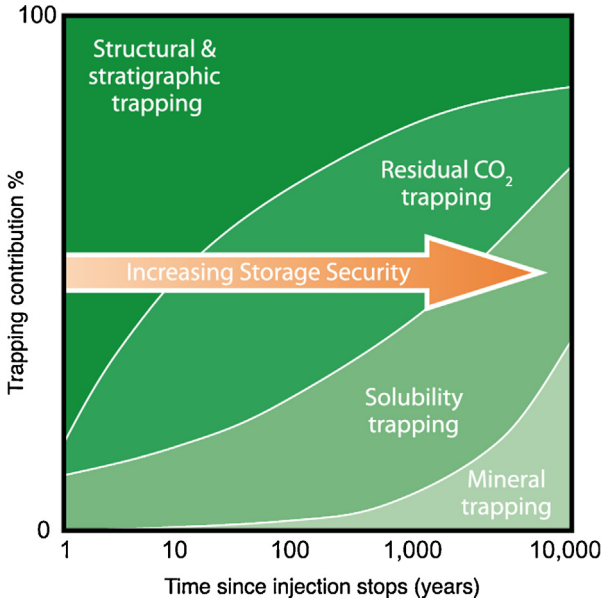

Fig. 2. A schematic of the relative importance of various trapping mechanisms over time, from Benson et al. (2005, 2012). Residual trapping is significant both in the amount of trapping capacity it provides as well as for the speed over which residual trapping takes place, simultaneously with water influx into the migrating plume.

this represents a major development in a relatively short period of time in the understanding of the importance of capillary trapping for CO_2 storage.

The structure of this review follows the spatial scales of interest to processes of capillary trapping, from the pore to the field. In Section 2 the pore scale processes underlying capillary trapping are discussed. Section 3 is a review of the theory and observations underlying the treatment of capillary trapping as a continuum property of rock-fluid system, described by the initial-residual constitutive relationship. Experimental techniques are discussed in detail in addition to a summary of observations reported in the literature covering a range of rock types and reservoir conditions. Section 4 concerns several issues of importance at the field scale. The findings of theoretical and numerical studies evaluating the impact of capillary trapping on plume migration, the role of residual trapping in regional storage capacity estimation, the emergence of engineering strategies to maximise capillary trapping and observations of residual trapping at field demonstration experiments are all reviewed in this section. Section 5 includes a brief discussion of two key outstanding uncertainties for capillary trapping, namely, trapping in mixed-wet systems and residual trapping incorporating the impacts of natural rock heterogeneity. Finally the conclusion summarises the key findings of the last ten years with regards to our understanding of capillary trapping and its importance for various aspects of the implementation of CO_2 storage.

2. Pore scale physics

The pore-scale mechanisms of fluid displacement, and specifically trapping, were first observed and described in two-dimensional micro-model experiments (see, for instance, Lenormand et al., 1983; Dullien, 1992). The principal application of the work was initially to understand waterflooding in oil reservoirs, where oil is trapped in the pore space, resulting in poor hydrocarbon recovery. Here we will apply the same concepts to storage. Initially the aquifer is full of brine and is, we assume, water-wet; this approximation is discussed later. Carbon dioxide invades the pore space as the non-wetting phase, preferentially filling the larger regions of the pore space, and leaving resident brine in the tighter, smaller pores and in the corners of roughness of the pore space. Capillary trapping occurs after this initial injection phase, when CO_2 migrates through the aquifer – at the trailing edge of the CO_2, water (brine) displaces CO_2, as shown in Fig. 1: this is an imbibition process which we will describe at the pore scale in detail below.

In micro-models displacement was observed in a lattice of wider void spaces (pores) connected by throats etched into glass. The pioneering work in this area was performed by Lenormand et al. (1983, 1988) supported by pore-scale modelling that explained the displacement processes and made predictions of the amount of trapping (Larson et al., 1981; Mohanty et al., 1987; Lenormand et al., 1988; Jerauld and Salter, 1990; Blunt and Scher, 1995; Øren et al., 1998; Valvatne and Blunt, 2004). The same concepts have also been applied to storage (Bandara et al., 2011). More recently, direct three-dimensional imaging of rock samples using synchrotron X-ray sources have confirmed some of the mechanisms previously observed in idealized systems (Coles et al., 1998; Berg et al., 2013; Armstrong and Berg, 2013; Georgiadis et al., 2013).

The amount of capillary trapping is determined by a competition between flow in wetting layers – the water that clings to the corners and roughness of the pore space (Ransohoff and Radke, 1988) – and frontal or piston-like advance, where water directly pushes out from the centre of the pore space. Here we describe each process in turn: frontal advance suppresses trapping, while wetting layer flow and the associated displacement, called snap-off (Roof, 1970), leads to a substantial degree of trapping. The overall amount of trapping

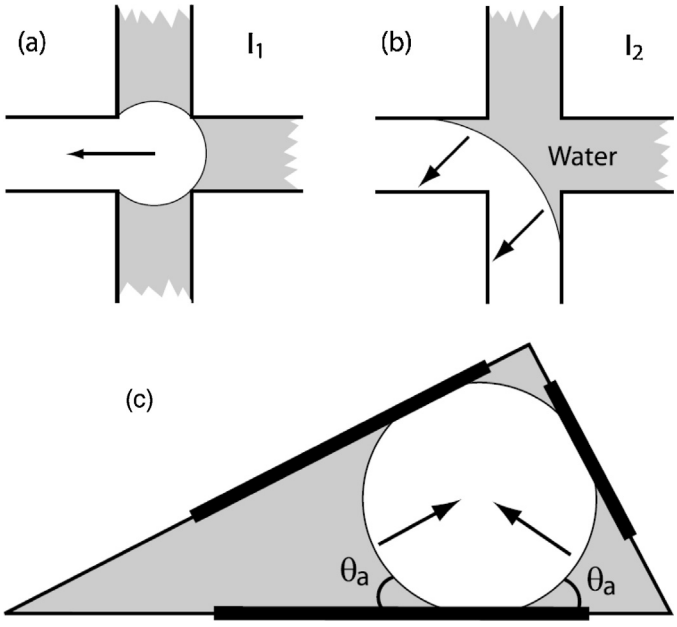

Fig. 3. Illustrations of wetting phase advance (imbibition). (a) We conceptualise a porous medium as comprising wide void spaces, pores, connected by narrower regions, called throats. Such a network can also be constructed to observe displacement processes. Here I_1 pore-filling is shown, where wetting phase (grey) displaces water from a pore with only one connected throat filled with non-wetting phase. The capillary pressure for the process is governed by the radius of curvature of the interface – here the displacement is favoured as the radius of curvature is relatively small. (b) The I_2 pore-filling process, where two surrounding throats are filled with the non-wetting phase. This is less favoured, as the critical radius of curvature for the displacement is larger. (c) Snap-off. Here a throat is shown in cross-section with an idealised triangular shape. Wetting phase resides in the corners of the pore space, with the non-wetting phase initially in the centre. As the water pressure increases, the wetting layers swell and the layers move across the solid surface with an advancing contact angle θ_a. When the non-wetting layers lose contact with the solid we have an unstable arrangement of fluid: the centre of the throat rapidly fills with wetting phase in a process called snap-off. Throats can be filled with water away from a connected wetting phase advance through the centres of pores and throats, allowing the non-wetting phase to become stranded or trapped in the larger pores. Figures taken from Valvatne and Blunt (2004).

is then controlled by the pore structure, flow rate, and wettability – the contact angle between the CO_2 and the solid surface (Jerauld and Salter, 1990; Blunt and Scher, 1995; Øren et al., 1998; Valvatne and Blunt, 2004).

2.1. Piston-like advance

We can consider the disordered pore space of a real rock in terms of an equivalent network of wide pore spaces interconnected by narrower throats, as shown schematically in Fig. 3. Frontal, or piston-like, advance is easy to understand for throats: an adjacent pore is filled with wetting phase which then pushes out the non-wetting phase from the centre of the throat. The wetting phase preferentially fills the narrowest regions of the pore space (the capillary pressure – the pressure difference between CO_2 and water – is highest, indicating that displacement can occur at a low imposed water pressure). Hence, filling a throat is favoured, while wetting phase advance will be impeded by larger pores.

A wetting phase front, on reaching a pore, will not spontaneously advance until the water pressure increases further. This may allow more throats connected to a given pore to be filled with water. This results in a cooperative process, where filling is increasingly favoured when more connected throats are already filled with wetting phase, shown in Fig. 3. The wetting phase has to traverse the pore – the displacement pressure is controlled by the largest radius of curvature needed to do this. When more adjacent throats

are filled with water, this critical radius of curvature is smaller and the displacement occurs at a higher capillary pressure, or for a lower water pressure. Using the terminology of Lenormand et al. (1983), we have imbibition pore-filling events labelled I_n, where n is the number of adjacent throats still filled with non-wetting phase. An I_0 event is not possible, as then non-wetting phase is already trapped (surrounded by water). The event I_1 is most favoured, followed by I_2; I_3 is rarely observed.

The result is to encourage a flat, frontal advance of the wetting phase with very little trapping – any invaginations in the invading front are more likely to fill by the I_1 mechanism than a protruding finger of water that will require an I_3-type process to advance. This type of uniform filling was first observed in micro-model studies (Lenormand et al., 1983) and also represents wetting phase invasion in, for instance, a uniform, dry sand, resulting in very little air (non-wetting phase) being trapped (Blunt and Scher, 1995).

2.2. Snap-off and wetting layers

There is one other important concept to consider for wetting phase displacement, one that controls capillary trapping: wetting layer flow and snap-off. As mentioned above, a storage aquifer is initially fully saturated with brine. When CO_2 is injected, it displaces brine as the non-wetting phase; the brine, however, is retained in the smallest regions of the pore space, and in the corners and roughness of the pore space. It is the brine in the corners or roughness of the pores that we call wetting layers – these are not molecular films (which may also coat the surface with a nanometre thickness) but bulk volumes of fluid micrometres thick that can allow significant flow.

During imbibition, as the water pressure increases, the wetting layers will swell, as shown in Fig. 3(c). If the advance of the water is slow – and it is predicted that in storage situations, the natural flow of brine may be only a few metres per year, then – at the micron scale – wetting layers will swell well in advance of the connected advance of water through the centres of pores and throats discussed previously. There comes a point when the non-wetting layers lose contact with the solid surface: this situation is unstable and the centre of the throat rapidly fills with water (Roof, 1970; Mohanty et al., 1987). In capillary equilibrium, this happens first at the narrowest point of the smallest throat: essentially throats can fill in order of size, with the smallest filling first in a percolation-like process (Dias and Wilkinson, 1986; Blunt and Scher, 1995). What about the pores? In this situation, all the surrounding throats can fill, surrounding and trapping the non-wetting phase in the pores. This then leads to a very large amount of trapping, since the pores contain the majority of the void volume in the rock.

The reality is a competition between piston-like advance and snap-off. An analysis of the critical capillary pressures shows that it is always more favourable to fill a throat by piston-like advance than by snap-off; hence snap-off only occurs if the wetting phase movement is significantly impeded by very large pores (Øren et al., 1998; Valvatne and Blunt, 2004). Overall, the degree of trapping is controlled by the wettability (more water-wet media allow more wetting layer flow and snap-off leading to more trapping), the ratio of pore to throat size (large pores and relatively smaller throats favour trapping) and connectivity (better connected pore spaces – that is where every pore is connected to many throats – makes trapping less likely). Increasing the flow rate also suppresses snap-off and trapping, since there needs to be sufficient time for the wetting layers to swell before the frontal advance of the wetting phase fills the pore space (Lenormand et al., 1983; Blunt and Scher, 1995). As discussed in Section 3.2, this effect is small until a critical flow rate (or capillary number) is reached.

2.3. Capillary trapping in the context of storage

While the basic notions of snap-off and trapping are well-established in the literature, the application to storage is not necessarily straightforward. We only expect significant trapping if the CO_2 is non-wetting and brine is the wetting phase, allowing layer flow and snap-off. However, while most storage aquifers are expected to be water-wet, chemical processes such as the dissolution of CO_2 could affect the surface properties and render the rock neutrally or even CO_2-wet. In this case, there is no snap-off and brine is likely to advance as a connected front with little or no trapping, which is concerning for long-term storage security, as could then move through the subsurface without leaving behind a safely stored trail of trapped ganglia.

As we discuss in the Section 3.2, contact angle measurements between CO_2 at storage conditions, where the CO_2 is in a dense super-critical phase, and brine on flat, pure mineral surfaces have been contradictory, with both water-wet and more neutrally wet conditions encountered (Hildenbrand et al., 2004; Chiquet et al., 2007; Yang et al., 2008; Chalbaud et al., 2009; Bikkina, 2011; Broseta et al., 2012). However, this is an indirect indication of the amount of trapping. Some capillary pressure measurements, however, have also suggested intermediate wettability for the CO_2-brine system (Plug and Bruining, 2007).

The use of three-dimensional X-ray micro-tomography (micro-CT scanning) of the pore space of rock was first presented by Flannery et al. (1987), with the first images of fluid distribution shown by Coles et al. (1998); subsequent developments in imaging and microfluidics technology now allow researchers to see fluid displacement inside the pore space of rock at micron resolution under reservoir conditions and determine, directly, how much CO_2 is trapped. This is a potentially revolutionary new technology with many applications; see Wildenschild and Sheppard (2013), and Blunt et al. (2013) for recent reviews.

In the context of CO_2 storage, the first micro-CT studies at elevated pressures were performed by Silin et al. (2011). Iglauer et al. (2011) and Andrew et al. (2013, 2014b) used an X-ray transparent carbon fibre core holder to maintain high temperatures (50–70°C) and pressures (around 10 MPa) in the fluids; these conditions are typical of many storage aquifers. They imaged the distribution of trapped super-critical CO_2, see Fig. 4. These results suggest that significant trapping is possible – up to two-thirds of the initial saturation is trapped for both sandstones and carbonates – indicating that CO_2 is the non-wetting phase. This result – significant trapping – is consistent with other experiments with super-critical CO_2 in unconsolidated porous media (Chaudhary et al., 2013; Pentland et al., 2010), core-scale experiments, where the average trapped saturation is measured (Pentland et al., 2011; Krevor et al., 2012; El-Maghraby and Blunt, 2012; Akbarabadi and Piri, 2013, see Section 3) and images of trapped phases at ambient conditions (see for instance, Karpyn et al., 2010; Georgiadis et al., 2013).

It is also possible to use pore-scale images to measure contact angle directly (Armstrong et al., 2012); for the supercritical CO_2-brine system, the contact angles have been measured on a calcite rich carbonate rock to lie in the range 40–50°, again confirming water-wet conditions (Andrew et al., 2014a). Furthermore, the size distribution of trapped ganglia obeys an approximate power-law distribution (Andrew et al., 2014b), consistent with percolation theory where throats are simply filled in order of size (Wilkinson and Willemsen, 1983; Blunt and Scher, 1995). Overall, it is now reasonable to assume that – at the pore scale – significant quantities of injected CO_2 will be trapped during post-injection migration through the aquifer, with the CO_2 acting as the non-wetting phase. Further work on imaging and modelling is needed to quantify this effect for different storage situations of interest and to combine

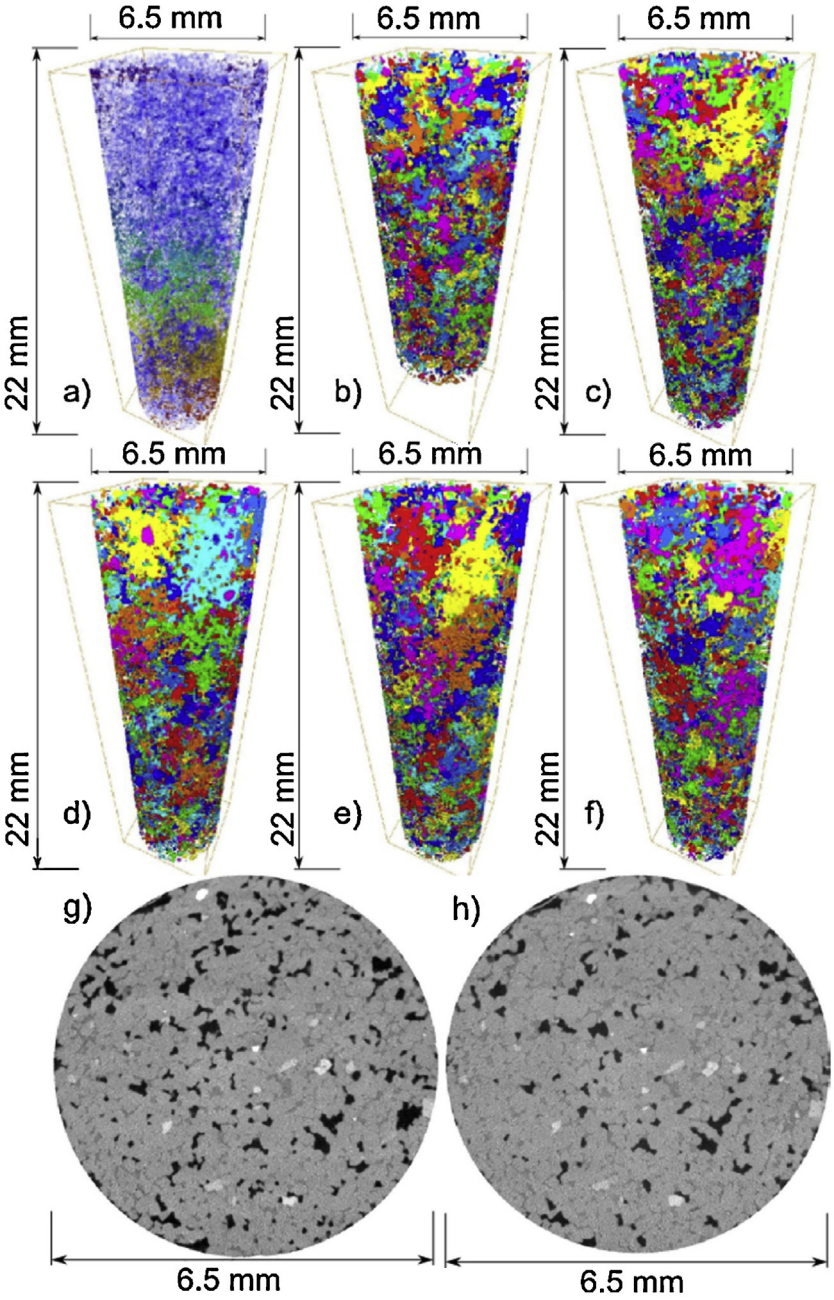

Fig. 4. Three-dimensional images of trapped CO_2 at typical storage conditions in a sandstone. (a) The distribution of CO_2 in the pore space after primary drainage (CO_2 injection). The colours indicate separate clusters of CO_2: most of the CO_2 is connected in one cluster that spans the sample and is shown in blue. (b)–(g) Trapped CO_2 images after the injection of brine for five replicate experiments. Here we see trapped ganglia of CO_2 of many sizes occupying approximately one third of the pore space. (h) and (i) are two-dimensional cross-sections of the raw three-dimensional images after drainage and brine injection respectively. The CO_2 is black, rock is the lightest phase and brine is intermediate. Figure taken from Andrew et al. (2014a). (For interpretation of the references to color in this figure legend, the reader is referred to the web version of the article.)

assessments of dissolution, capillary and mineral trapping simultaneously.

3. The rock core and constitutive relationships for flow modelling

The complex processes described in Section 2 averaged over tens of thousands of pores give rise to the residually trapped CO_2 saturation. This is the basis of rock core analysis for reservoir characterisation and flow modelling. At the scale of centimetres or larger, a general definition of the residual saturation of a non-wetting fluid is the asymptotic saturation achieved with increasingly negative capillary pressure (Anderson, 1987a; Morrow, 1990). This is illustrated in Fig. 5 for water-wet and mixed-wet CO_2-brine systems. This is the irreducible CO_2 saturation obtained with increasing pore volumes and/or velocity of water flowing through the rock. The residually trapped saturation is not a single valued parameter of the rock, however, and a constitutive relationship – the initial-residual curve – is commonly used to describe the residual trapping character of a rock. This relationship is also the basis for incorporating the hysteresis of flow functions into reservoir modelling. These concepts along with the published data for CO_2-brine systems are reviewed in this section.

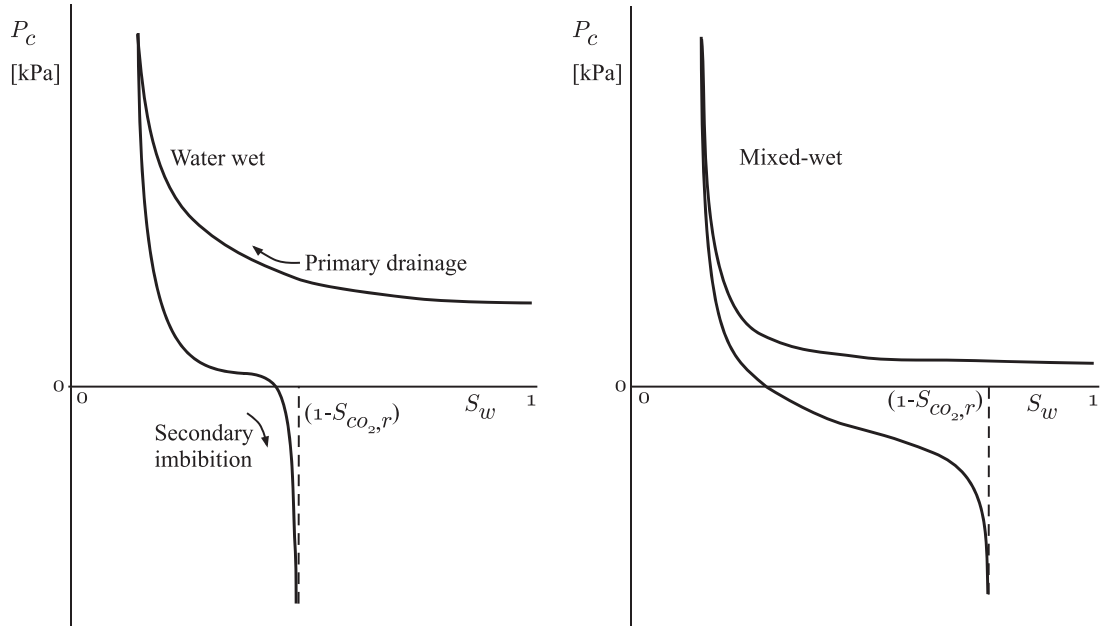

Fig. 5. Capillary pressure curves showing the processes of primary drainage and secondary imbibition. The definition of the residually trapped CO_2 saturation is shown as the limit of CO_2 saturation achieved at increasingly negative capillary pressure. For the water-wet case, the residual is nearly achieved by $P_c = 0$ during imbibition, whereas for the mixed-wet case substantial CO_2 desaturation occurs at negative values of capillary pressure.

3.1. The initial-residual characteristic curve

The residually trapped saturation is dependent on the CO_2 saturation before water imbibition – the larger fraction of pores initially filled with CO_2, the more snap-off and trapping will occur as brine invades the pore space. The relationship between the initial and residual non-wetting saturations is known as the *IR* (for initial-residual) curve and and a number of empirical models have been developed around this concept. Reviews included in Pentland et al. (2010) and Joekar-Niasar et al. (2013) discuss the models developed by Land (1968), Lenhard and Parker (1987), Ma and Youngren (1994), Jerauld (1997), Kleppe et al. (1997) and Spiteri et al. (2008). In short these models take different functional forms and have either one or two degrees of freedom with which to match observed data.

For illustration, the *IR* model proposed by Land (1968) is given by

$$S^*_{CO_2,r} = \frac{S^*_{CO_2,i}}{1 + CS^*_{CO_2,i}}, \quad (1)$$

where the CO_2 saturation, S_{CO_2}, is scaled by the irreducible water saturation, $S_{w,irr}$, to obtain the normalised CO_2 saturation, $S^*_{CO_2} = S_{CO_2}/(1 - S_{w,irr})$. The *IR* curves for various values of *C* are shown in Fig. 6. With this model the residual CO_2 saturation is an increasing function of the initial saturation prior to imbibition, but the slope decreases with increasing initial saturation. This reflects a decreasing marginal effectiveness of trapping with increasing initial saturation because the higher saturations are achieved through the invasion of increasingly small pores. This is a common, although not general characteristic of *IR* models. The model of Spiteri et al. (2008), for example, was constructed to allow non-monotonic *IR* profiles, sometimes a feature of mixed-wet systems.

Like the other constitutive relationships describing multiphase flow, capillary pressure and relative permeability, the *IR* characteristic of a rock is considered to be invariant across a wide range of fluid pairs and conditions of temperature, pressure and brine salinity so long as the wetting state of the system is similar between systems. It is well known that the properties will vary, however, if these conditions control the wetting state of the system (Salathiel, 1973; Wang, 1988) or the flow velocity v, viscosity μ and interfacial tension σ combine in a way such that the dimensionless capillary number, $N_c = v\mu/\sigma$, exceeds a critical value for desaturation. For Berea sandstone, for example, this has been observed to be in the range $N_c > 10^{-5} - 10^{-4}$ (Taber, 1969; Foster, 1973; Gupta and Trushenski, 1979). For natural rocks representative of a wide variety of pore structures the range of capillary numbers for desaturation extends to $N_c > 10^{-7} - 10^{-4}$ (Lake et al., 2014).

Observations of the wetting state of the CO_2 brine system have raised doubts about whether these general observations extend to CO_2 displacement. Contact angle, conventionally measured in the wetting phase, water, was observed to increase (weakening water-wetting) with pressure by Broseta et al. (2012), Chiquet et al. (2007), Iglauer et al. (2014b), Jung and Wan (2012), Saraji et al. (2013), Wesch et al. (1997) but not by Espinoza and Santamarina (2010), Farokhpoor et al. (2013), Wang et al. (2013), Al-Menhali and Krevor (2013). Similarly contact angle was observed to increase significantly with brine salinity by Espinoza and Santamarina (2010), Jung and Wan (2012) but not by Broseta et al. (2012), Chiquet et al. (2007), Al-Menhali and Krevor (2013). Farokhpoor et al. (2013), Saraji et al. (2013) investigated the dependency of contact angle on temperature but a clear trend was not observed. A recent review of the subject (Iglauer et al., 2014a) highlights the challenging nature of these experiments and summarises that the wide range of behaviour observed can be attributed largely to differences in surface roughness and surface contamination between studies. Recent work reported in Niu et al. (2015), and discussed in further detail in the next section clearly demonstrate that these effects do not manifest in the *IR* curve for a sandstone, which remains constant across a wide range of test conditions.

Recent work focused on CO_2 storage has summarised the residual trapping relationship with a single value, the residual trapping efficiency, $R = S_{CO_2,r}/S_{CO_2,i}$ (Akbarabadi and Piri, 2013; Bachu, 2013; Burnside and Naylor, 2014).

For a given rock, this value, however, will depend strongly on the initial CO_2 saturation prior to imbibition. For example, using the

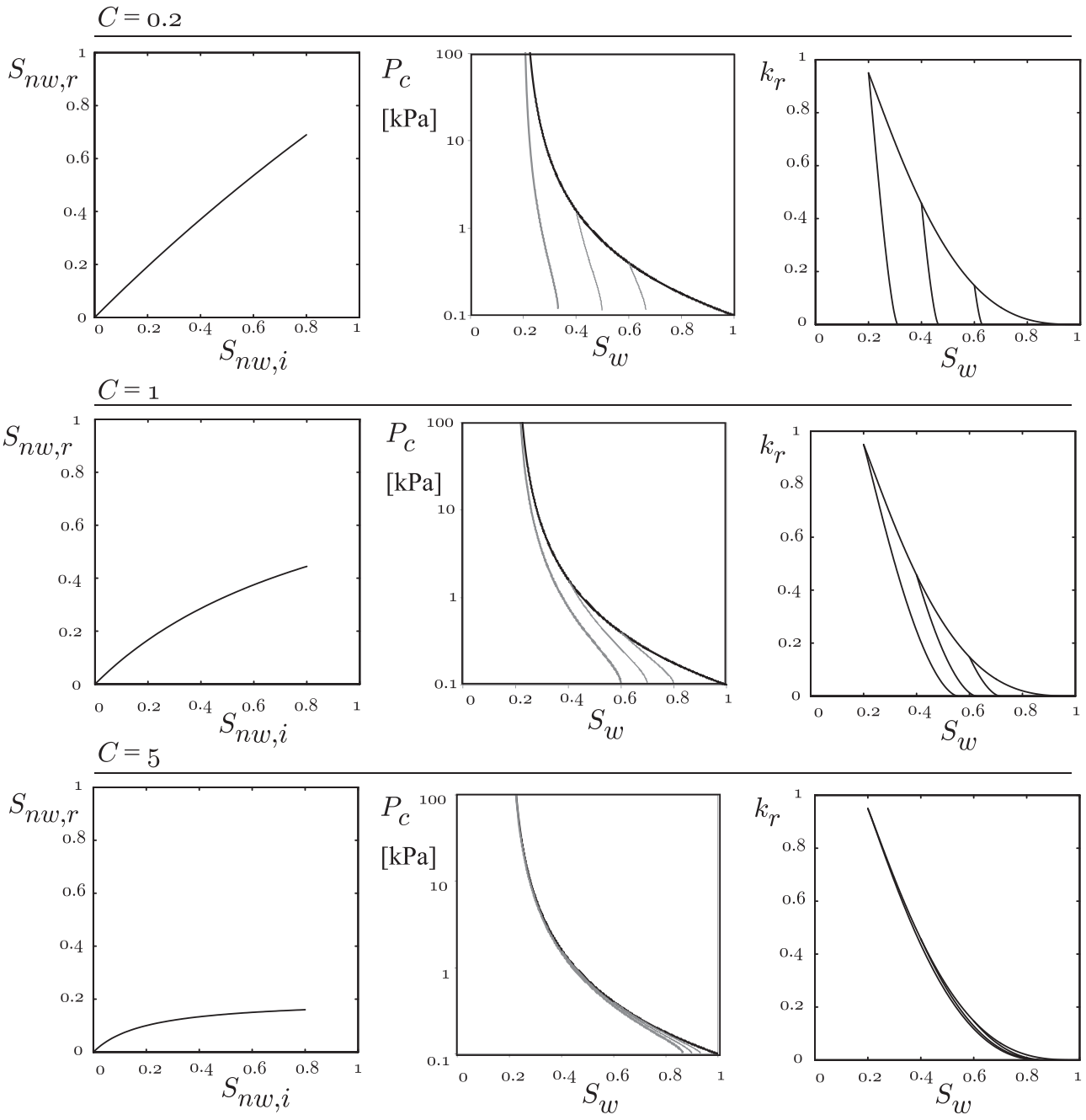

Fig. 6. The graph on the left shows *IR* characteristic residual trapping curves using the model of Land (1968) for various values of the constant *C*, Eq. (1). In the central and right columns imbibition curves departing from the primary drainage curves are shown for the values of *C* for the capillary pressure (Eq. (3)) and relative permeability characteristic curves respectively (Eq. (2)).

Land model (Eq. (1)) with a value of $C = 1$, the efficiency for a single rock would vary from 1 to 0.5 as the initial saturation varied from 0 to 1. Thus there is little basis for comparison of the residual trapping efficiency between rocks or reservoir conditions if the data is not first normalised to the initial saturation at which it was obtained. This has significantly limited the utility of cross-laboratory data evaluations when this information is not available or when initial saturations before imbibition vary widely (Bachu, 2013; Burnside and Naylor, 2014). This is particularly the case for CO_2-brine experiments where maximum saturations observed prior to imbibition are usually controlled by the arbitrary limitations of the experimental apparatus, rather than an intrinsic property of the rock such as the irreducible water saturation (Pini and Benson, 2013).

3.2. Residual trapping and hysteresis in multiphase flow

The residual trapping *IR* constitutive relationship has importance for reservoir characterisation beyond quantifying the magnitude of trapping. Since the work of Naar and Henderson (1961) and Land (1968) the most widely used continuum approaches for modelling multiphase flow in water-wet systems have assumed that residual trapping can be used to parameterise models for hysteresis in relative permeability and capillary pressure. In this approach, the non-wetting phase saturation, S_{nw} is conceptualised as consisting of parts that are *connected*, $S_{nw,c}$, contributing to flow and parts that are *disconnected*, $S_{nw,d}$, not contributing to flow. Thus $S_{nw} = S_{nw,c} + S_{nw,d}$ and $S_{nw,c} \leq S_{nw}$. The disconnected phase saturation is equivalent to the residual saturation

when $S_{nw,c} = 0$. It is assumed that relative permeability to the non-wetting phase, $k_{r,nw}$, is a function only of the connected saturation. Along a bounding drainage curve all of the non-wetting phase is assumed to be connected, $S_{nw} = S_{nw,c}$, whereas on an imbibition curve the connected saturation must be calculated from a model that uses observations of residual trapping for its parameterisation.

Models for hysteresis consist of: (i) a relationship between the relative permeability of the non-wetting phase and its connected or flowing saturation; (ii) a relationship between the capillary pressure and the connected or flowing non-wetting phase saturation; (iii) a model for the connected saturation as a function of saturation history; and (iv) a model that relates the disconnected, residual, saturation of the non-wetting phase to the maximum saturation obtained before imbibition.

The fourth component concerning the residual trapping is the observation based input into the parameterisation of hysteresis. Imbibition bounding or scanning curves can be used interchangeably with observations of residual trapping to constrain these models but there is an implied self-consistency. Specified imbibition curves imply an *IR* relationship and vice versa. Alternatively, both imbibition and residual trapping can be used to further parameterise the shape of the imbibition curves, the approach followed by the widely used model of Killough (1976). We emphasise again that all of these models are inherently empirical and as of yet the particular model or choice of parameters cannot be estimated from theoretical considerations, e.g., of the rock structure and wetting properties (see the discussion in Section 2 on pore scale physics).

For illustrative purposes we make use of one of the earliest and simpler models for residual trapping and imbibition relative permeability in water-wet systems, suggested by Land (1968) and similar to the approach employed for modelling CO_2 storage in Kumar et al. (2005) and Qi et al. (2009). In this version, the imbibition relative permeability to CO_2, $k^i_{r,CO_2}(S_{CO_2})$, at a given saturation, S_{CO_2}, is set as equivalent to the drainage relative permeability function, k^d_{r,CO_2}, evaluated at the connected saturation,

$$k^i_{r,CO_2}(S_{CO_2}) = k^d_{r,CO_2}(S_{CO_2,c}). \quad (2)$$

We add to this an illustration of water-wet capillary pressure hysteresis following the same approach, where $p^i_c(S_{CO_2})$, the imbibition capillary pressure at a given saturation is set as equivalent to the drainage capillary pressure function, $p^{dr}_c(S_{CO_{2,c}})$, evaluated at the connected phase saturation,

$$p^i_c(S_{CO_2}) = p^{dr}_c(S_{CO_{2,c}}). \quad (3)$$

This model assumes that the residual is obtained at a $P_c = 0$ and is not applicable to, e.g., mixed-wet systems.

The connected saturation can be obtained by the model proposed in Land (1968),

$$S^*_{CO_2,c} = \frac{1}{2}\left[(S^*_{CO_2} - S^*_{CO_2,r}) + \sqrt{(S^*_{CO_2} - S^*_{CO_2,r})^2 + \frac{4}{C}(S^*_{CO_2} - S^*_{CO_2,r})}\right]. \quad (4)$$

The parameter C is found by fitting an empirical relationship correlating the scaled residual saturation, $S^*_{CO_2,r}$, to the maximum initial scaled saturation of the CO_2, $S^*_{CO_2,i}$ prior to the imbibition process that led to trapping, Eq. (1). Thus, the *IR* curve is often the empirical basis for parameterising hysteresis in flow modelling.

The *IR* curves for a range of values of the Land constant C and the corresponding tracking hysteresis curves are shown for capillary pressure and relative permeability relationships in Fig. 6. As the value of the constant increases, trapping decreases and there is necessarily less hysteresis in the capillary pressure and relative permeability functions.

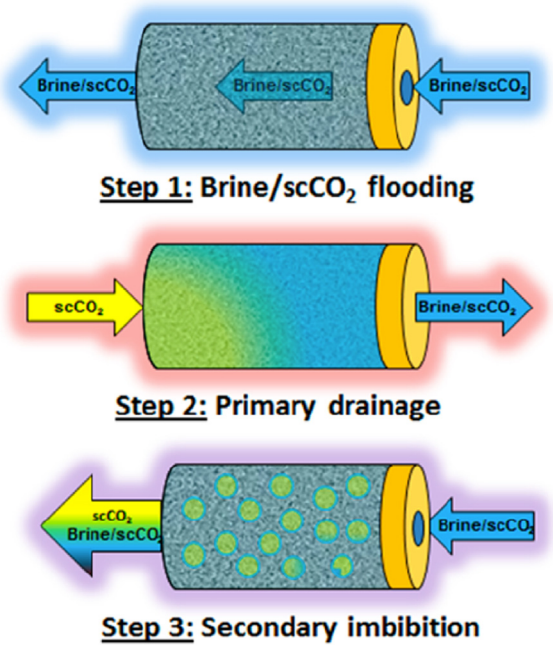

Fig. 7. A schematic showing the principles of the technique used in (Pentland et al., 2011; El-Maghraby and Blunt, 2012). Step 1 is the initial saturation of the rock sample with CO_2 saturated brine. Step 2 is the primary drainage displacement of CO_2 saturated brine by an immiscible CO_2 phase. Step 3 is secondary imbibition where a CO_2 saturated brine phase is injected into the rock sample displacing and trapping the CO_2 phase. Figure taken from El-Maghraby and Blunt (2012).

3.3. Core-scale measurements of trapping

The initial-residual relationship is typically observed during core-flooding (cm-scale) experiments in which liquid and gas phases are injected axially through a cylindrical rock sample – the rock core – that is confined in the radial direction to prevent fluid bypassing. Whether the phases are injected sequentially or simultaneously, the pressure and flow rate boundary conditions at the sample inlet and outlet, and the saturation measurement techniques can all vary resulting in different types of core flooding experiments; many of which have been employed historically in the context of hydrocarbon recovery. Here we focus on the two primary core-flooding methods used for CO_2-brine *IR* observations.

Early observations of residual trapping with supercritical CO_2 were reported by Suekane et al. (2008, 2009). The first characterisation of the CO_2-brine *IR* curve in sandstone (Pentland et al., 2011), and later in carbonate rock (El-Maghraby and Blunt, 2012), was made using a modified porous plate (semi-permeable disk) method. In this work a low permeability ceramic plate impervious to CO_2 was placed at one end of the rock sample, Fig. 7. The addition of the porous plate allowed precise control over the primary drainage flow sequence with a uniform distribution of connected CO_2 introduced into the rock sample at a known capillary pressure. The porous plate was modified by adding a central bypassing flowline which allowed the subsequent secondary imbibition flow sequence to be performed to reach residual saturation conditions (Pentland et al., 2014). The rock sample and porous plate were housed in a Hassler type core-holder (after Hassler and Brunner (1945)) which was connected to the necessary pumps and reactors. Saturations were measured by volume balance. The porous plate method was also used to make the first CO_2-water capillary pressure observations (Plug and Bruining, 2007). While this method allows for precise control of capillary pressures during primary drainage the attainment of capillary equilibrium can be time consuming, especially for low permeability rocks.

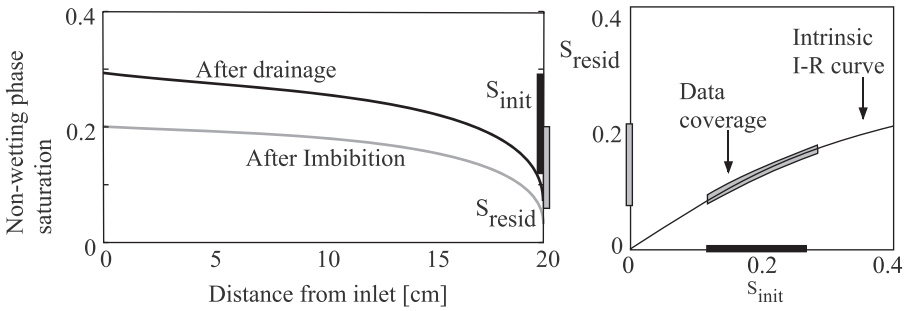

Fig. 8. A schematic showing the principles of the core flood technique used in (Niu et al., 2015) for the rapid construction of the residual trapping curve. A drainage core flood is performed and X-ray imaging used to obtain saturation along the core (left). Using drainage flow rates that optimise the capillary end effect, a range of initial CO_2 saturations can be imaged in the core prior to imbibition. Upon imbibition the saturation lowers and the *IR* curve is constructed (right) correlating the final saturation in each slice along the core to the saturation prior to imbibition.

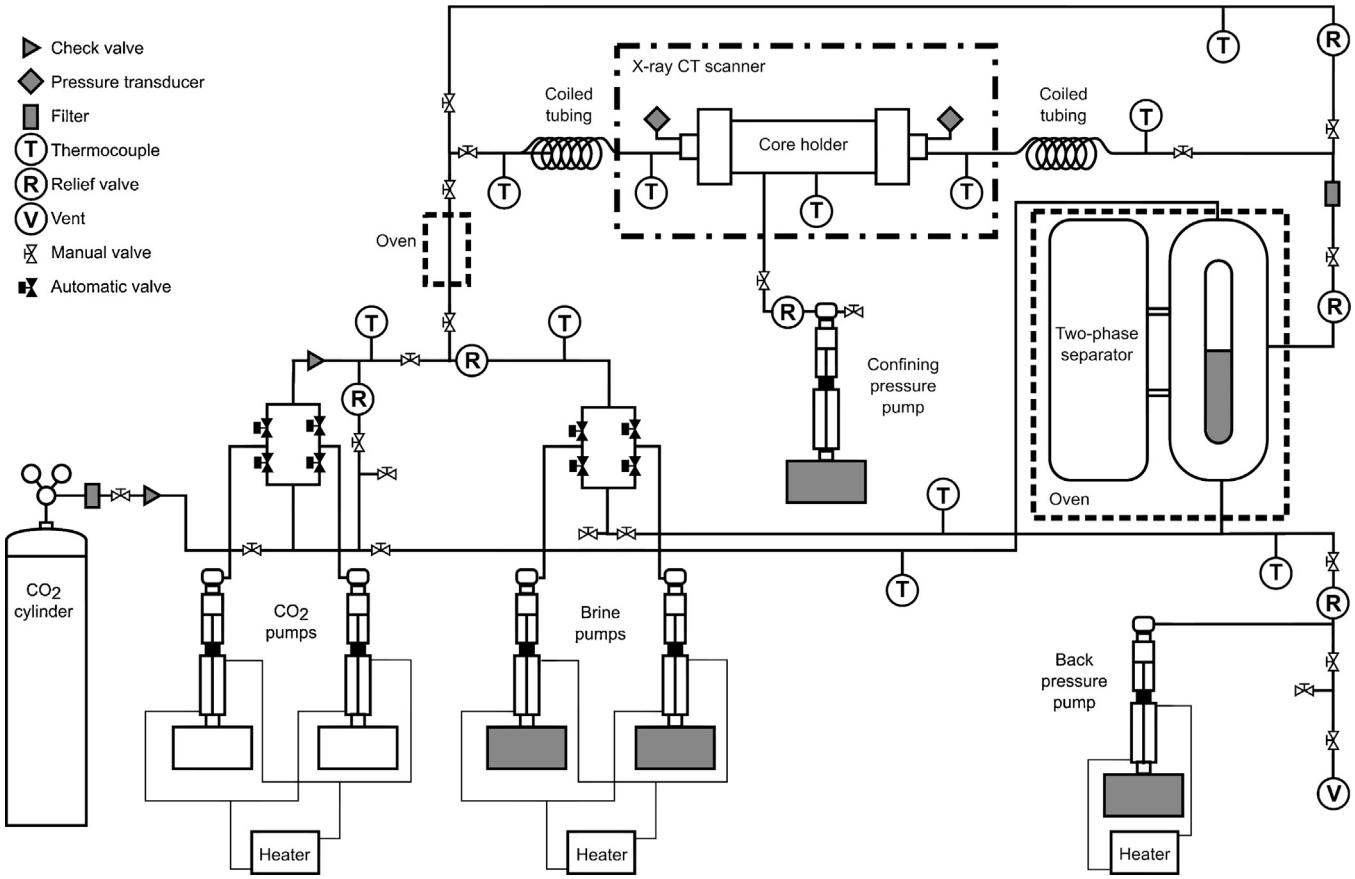

Fig. 9. Schematic of an experimental apparatus for coreflooding with in situ saturation monitoring used in Reynolds et al. (2013) and Niu et al. (2015).

More observations of the *IR* relationship have been made using a steady-state core-flooding method in which the CO_2 and aqueous phases were co-injected into the rock sample at known volume fractions (Shell, 2011; Shi et al., 2011a,b; Lu et al., 2012; Krevor et al., 2012; Akbarabadi and Piri, 2013, 2015; Ruprecht et al., 2014; Zuo and Benson, 2014; Niu et al., 2015; Li et al., 2015). Typically a constant pressure outlet boundary condition and a constant total flow rate inlet boundary condition were maintained while saturations were measured in situ using medical X-ray computed tomography. By varying the fractional flow of the two phases while imaging the average saturation along the core, the *IR* relationship could be determined, Fig. 8. This method typically requires careful phase equilibration and fluid re-circulation due to the large number of fluid volumes passing through the sample. This demands a more complex set of peripheral pumps, reactors and a phase separator – compare the experimental apparatus used in El-Maghraby and Blunt (2012) with that of Niu et al. (2015) shown in Fig. 9.

3.4. Observations of trapping with CO_2-brine systems

A large number of observations of residual trapping of supercritical CO_2 have been reported over the last 10 years. Fig. 10 is a compiled *IR* plot of literature data for CO_2-brine systems at pressures and temperatures above the critical point for CO_2. Curves using the Land model (Eq. (1)) with approximate bounding values of the constant C show an overall range of $0.2 < C < 5$ (Bennion and Bachu, 2008, 2010; Pentland et al., 2011; Shi et al., 2011a; Shell, 2011; Smith et al., 2011; Krevor et al., 2012; El-Maghraby and Blunt, 2012; Lu et al., 2012; Akbarabadi and Piri, 2013; Bachu,

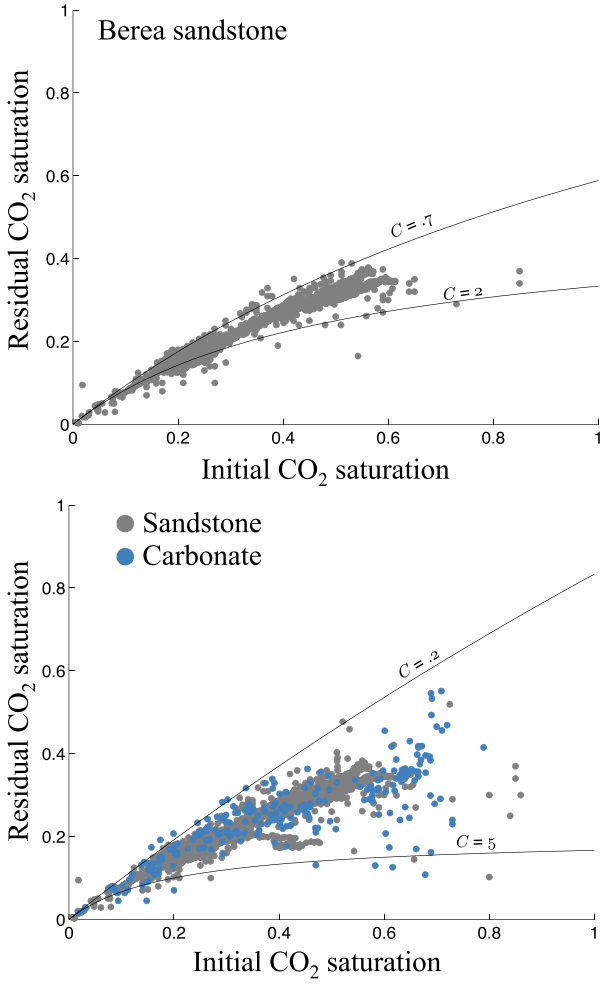

Fig. 10. The upper plot shows reported observations of residual trapping with supercritical CO_2 made on Berea sandstones. The lower graph shows all of the data in the literature for residual trapping with supercritical CO_2 with the colouring distinguishing between sandstone and carbonate rocks. The solid lines show Land model curves with approximate 95% bounds on the data. See text for references.

2013; Ruprecht et al., 2014; Zuo and Benson, 2014; Niu et al., 2015; Li et al., 2015). A searchable database including various attributes of the tests – rock properties, experimental conditions – is available online as supporting information.

One simple but important conclusion that can be drawn from the combined dataset is that the saturation of residually trapped CO_2 is likely to be at least 10% of the pore volume and many rocks are capable of residual trapping at saturations between 30 and 40% of the pore volume, depending on the rock and initial saturation before imbibition.

Analyses of other aspects of the combined dataset reported in Bachu (2013) and Burnside and Naylor (2014) found no correlation between reservoir conditions or other multiphase flow properties (e.g., drainage relative permeability) and the *IR* characteristics which were evidently controlled by the unique pore structure of a given rock type, or indeed particular rock sample. The comparison of sandstone and carbonate *IR* data in Fig. 10 reinforces this conclusion – the main discernible difference is the wider scatter of the carbonate rock data, likely due to the greater level of heterogeneity in the carbonate rocks that have been tested.

A number of the studies have targeted important fundamental questions about the nature of trapping in the CO_2-brine system. The upper plot of Fig. 10 shows the compiled set of observations made with Berea sandstone, reported by several different research groups with various experimental techniques at a range of conditions (Pentland et al., 2011; Shi et al., 2011a; Krevor et al., 2012; El-Maghraby and Blunt, 2012; Akbarabadi and Piri, 2013; Ruprecht et al., 2014; Zuo and Benson, 2014; Niu et al., 2015; Li et al., 2015). There is a notable consistency among the reported observations suggesting that the *IR* characteristic of a rock is robust against variations in reservoir conditions and, to a certain extent, experimental technique.

The impact of reservoir conditions was evaluated directly in Niu et al. (2015). It was found that varying pressure 5–20 MPa, temperature 25–50°C, and brine salinity 0–5 mol/kg NaCl, had no impact on the residual trapping characteristic of Berea sandstone. Any change in the wetting state of the system was not significant enough to effect trapping. The *IR* curves for CO_2-brine systems were also indistinguishable from the *IR* curve measured with the water wet N_2-water system.

An inspection of the transient saturation profiles during imbibition reported in several studies also showed that the residual CO_2 saturation in sandstone rocks was obtained quickly, with less than one pore volume of brine injected (Shell, 2011; Shi et al., 2011a,b; Lu et al., 2012; Akbarabadi and Piri, 2013; Niu et al., 2015). This rapid desaturation is characteristic of a water-wet system when the viscosity ratio of the displacing fluid to displaced fluid is high, as is the case with brine displacing CO_2. Mixed-wet systems would require many more pore volumes of brine before the residual was achieved (Salathiel, 1973).

The stability of the residually trapped phase has also been demonstrated in the laboratory, with CO_2 remaining immobile for at least 10 and up to 100 pore volumes of brine injected (Shi et al., 2011a,b; Niu et al., 2015; Lu et al., 2012; Akbarabadi and Piri, 2013). This represents decades or longer in subsurface reservoirs with fluid velocities typical of engineered or natural processes.

Beyond these largely theoretical studies, a number of observations of the residual trapping characteristics of CO_2-brine-rock systems on real reservoir rocks have been reported. These studies were performed to obtain the trapping characteristics, or single data points for trapping at a real or nominally representative reservoir condition. The most extensive dataset comes from the individual trapping data points (pairs of S_i, S_r) for sandstones and carbonate rocks from target sequestration reservoirs in the Alberta Basin, Canada (Bennion and Bachu, 2008, 2010; Bachu, 2013). In these rocks trapping saturation ranged from 20- 60% and corresponded to a range of Land constants $0.18 < C < 2.2$.

Outside of Canada, characteristic trapping curves have been published for sandstone rocks from pilot CO_2 storage sites in the United States (Krevor et al., 2012; Lu et al., 2012), Australia (Krevor et al., 2012), and target storage reservoirs in the UK (Smith et al., 2011; Shell, 2011). Land constants range from $1 < C < 2$. In these cases all of the rocks were sandstones with well connected pore space and were homogenous at the scale of the core, as compared with typical carbonate rocks.

The main conclusions to draw from these analyses are that residual trapping will be a significant trapping mechanism for CO_2 storage, unaffected by reservoir conditions, typical of water-wet systems, and stable over timescales of decades to a century if not longer. The nature of residual trapping is most suitably characterised by the *IR* curve which will be highly specific to the reservoir of interest. These conclusions are consistent with the pore-scale observations described in Section 2.3.

4. Capillary trapping at the reservoir scale

The interest in capillary trapping for CO_2 storage comes largely from the impacts that this process has as it occurs over the extent of the migrating CO_2 plume. It was reservoir scale modelling that

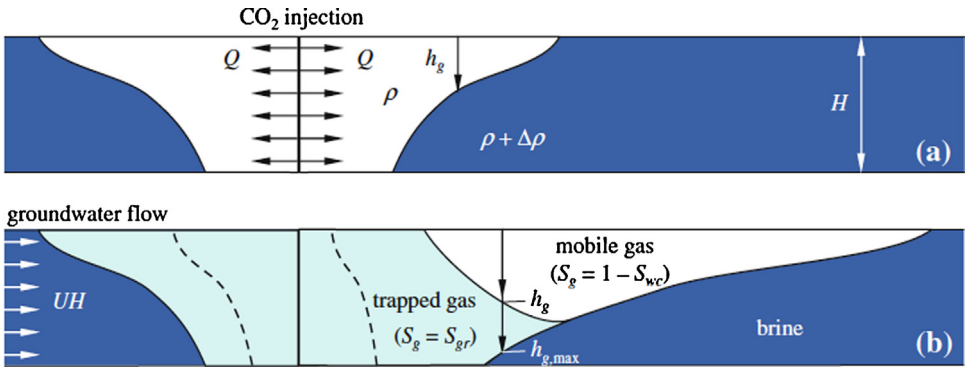

Fig. 11. A schematic taken from Juanes et al. (2010) showing an example of a sharp interface model with the major defining characteristics: the model is two dimensional, allows for three values of saturation and includes an initial injection condition in which injection is uniform across the entire height of the reservoir body. In these models the residually trapped saturation takes on a single value and the total trapping is simply proportional to the reservoir sweep of the plume.

initially demonstrated that capillary trapping was a feature likely to have a major impact on CO_2 storage security and reservoir management (King and Paterson, 2002; Doughty and Pruess, 2004). This has resulted in residual trapping characteristics of reservoirs playing a key role in national storage capacity estimates, the development of reservoir management strategies to enhance residual trapping, and several tests in which the existence and stability of residual trapping was observed at the field scale.

4.1. Modelling the impact of capillary trapping at the field scale

Various theoretical models have been developed to provide first order estimates of the impact of the salient features of CO_2 migration in a reservoir during injection and after injection has completed. Most of these models incorporate capillary trapping and they provide a clear link between the residually trapped CO_2 saturation and limits on flow extent and storage capacity (Hesse et al., 2008; Farcas and Woods, 2009; Gasda et al., 2009; Juanes et al., 2010; Hesse and Woods, 2010; MacMinn et al., 2010, 2011; Nordbotten and Dahle, 2011; Golding et al., 2011, 2013). This approach, based in the field of fluid mechanics, and many of the models are the subject of a recent review in Huppert and Neufeld (2014). Theoretical models are generally two dimensional. They depend on the assumption that the pressure distribution is hydrostatic and that fluid migration is dominated by lateral movement.

The first set of such models developed were the *sharp interface* models, where CO_2 saturation, S_g, was either at a maximum, $S_g = 1 - S_{wc}$, where S_{wc} is the connate water saturation, or at a single residual saturation, S_{gr} (Hesse et al., 2008; Farcas and Woods, 2009; Gasda et al., 2009; Juanes et al., 2010; Hesse and Woods, 2010; MacMinn et al., 2010, 2011). A schematic for the model proposed in Juanes et al. (2010) is shown in Fig. 11. This is a significant simplification from the known physics of the *IR* relationships described in Section 3 but even so the effect of residual trapping on the migration of the plume is significant. In particular, as a plume (that is, the mobile component of the CO_2) migrates and water subsequently imbibes the trailing end, the plume decreases in size as residually trapped CO_2 is lost during migration. Eventually the entire plume is consumed by this process resulting in constraints on the total distance and time over which a plume may migrate. Despite their simplicity, these models are able to incorporate effects of background hydrologic flow and confining layer slope. These models show that the extent of microscopic residual trapping is as important to speed and distance over which a plume travels as any of the other parameters in the model, e.g, confining layer slope and rock permeability. In this way it has been demonstrated that residual trapping brings the significant supplementary benefit of minimising the distance and speed of plume migration.

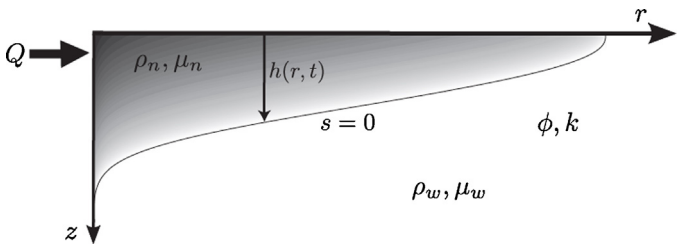

Fig. 12. A schematic from Golding et al. (2013) showing an example of a theoretical model evaluating the impacts of the capillary fringe on CO_2 plume movement. In this model a range of saturations are allowed corresponding to the capillary pressure characteristic curve. In the figure, saturations are in grey scale, with white corresponding to zero CO_2 and black corresponding to the maximum CO_2 saturation at the irreducible water saturation. Capillarity leads to an increased sweep, lower average saturation and overall increased residual trapping relative to models ignoring capillarity.

A second group of theoretical models has been developed more recently that are able to account for the impacts of capillarity. These models allow for a nonuniform saturation in the plume and find solutions for the case where capillary pressure is controlled by buoyant effects. Specifically, the distinct densities of the fluids give rise to separate hydrostatic pressures with plume height, giving rise to an increasing capillary pressure with plume depth. These are called *capillary fringe* models (Nordbotten and Dahle, 2011; Golding et al., 2011, 2013). A schematic of one such model from Golding et al. (2013) is shown in Fig. 12. These models have shown that the plume shape was significantly affected by the presence of capillarity. Increasing the strength of capillary effects – higher entry pressure, larger pore size distribution – lead to a significant increase in sweep of a gravity current. Due to the capillary fringe the plume saturation in these models is on average lower than in a sharp interface model. In all cases the increased sweep of the plume had a larger impact than the reduced saturation on trapping and the total residual trapping was always higher when capillarity is considered (Golding et al., 2011). Thus in addition to increasing the sweep and slowing the current, capillarity serves to increase the fraction of CO_2 residually trapped, leading to further decreases in plume migration as mobile CO_2 is lost to residual ganglia.

Numerical studies simulating the injection and migration of CO_2 into reservoir geometries more representative of target geologic systems have largely confirmed the findings of the theoretical models (King and Paterson, 2002; Pruess et al., 2003; Flett et al., 2004; Kumar et al., 2005; Juanes et al., 2006; Doughty, 2007; Doughty et al., 2008; Class et al., 2009; Eigestad et al., 2009; Goater et al., 2013). Specifically, the models have shown that variation in the trapping strength has a significant impact on plume migration, that residual CO_2 trapping can result in a complete trapping of CO_2

within the permeable part of the reservoir and that it is at least as important for plume immobilisation as the dissolution of CO_2 over time scales of hundreds of years.

These studies have also concluded that the properties of multiphase flow hysteresis, parameterised by the *IR* trapping curve, have first order impacts on plume migration, especially in the presence of the types of rock heterogeneity pervasive in reservoirs (Juanes et al., 2006; Doughty, 2007; Doughty et al., 2008). In particular, the incorporation of full hysteresis models results in a reduction in mobility for the parts of the plume that are undergoing imbibition relative to the parts of the plume draining the pore space. As a result, the plume tends to spread more in simulations that incorporate the full impact of hysteresis.

4.2. Residual trapping and national storage capacity estimates

The various effects of residual trapping on plume migration identified by the theoretical and numerical models has led to the incorporation of residual trapping in modelling used for the capacity estimation methodologies developed for several countries (Gammer et al., 2011; Halland et al., 2011; Szulczewski et al., 2012; Warwick et al., 2013). Regional storage capacity estimates often use the concept of storage efficiency for their evaluation – a topic that is the focus of the review paper of Bachu (2015) in this volume.

In the United States, for example, the USGS capacity estimate methodology (Warwick et al., 2013) calculates probably distributions of storage efficiency for individual reservoirs. These probabilities are generated by inputting ranges of values for reservoir properties, including the residually trapped gas saturation, into the sharp-interface model of Juanes et al. (2010). From this analysis it has been estimated that over 95% of the capacity for CO_2 storage in the United States is in the form of residually trapped CO_2.

The capacity estimates discussed in Gammer et al. (2011), Halland et al. (2011) for the North Sea in Norwegian and UK territory respectively, use reservoir simulation to evaluate the potential for storage in offshore reservoirs. In both cases, residual trapping plays a significant role. In the UK 65% of the total capacity is through storage in open reservoirs where residual and dissolution trapping are entirely responsible for the immobilisation of the plume.

4.3. Engineering capillary trapping

Injection can be engineered to enhance or speed up trapping (King and Paterson, 2002; Juanes et al., 2006; Cameron and Durlofsky, 2012). One way to achieve optimal trapping is to plan the injection site, location of the well and injection rates such that the plume will naturally migrate, under the influence of buoyancy and in the presence of a natural groundwater flow; as the CO_2 moves, it will leave behind a trail of trapped ganglia. However, the injection needs to be carefully planned, modelled and monitored to prevent the CO_2 escaping to the surface.

Large open aquifers potentially provide promising storage targets: as mentioned above, in the North Sea they comprise the majority of the available storage space (Goater et al., 2013). These aquifers do not have a complete geological seal; instead they have layers which may extend hundreds of kilometres to the sea bed, as shown in Fig. 13. After injection, the CO_2 will migrate under the combined influence of buoyancy and local groundwater flows. However, CO_2 will be rendered immobile – at the large scale – under local traps on the top surface of the aquifer and, more extensively, by capillary trapping as it migrates away from the injection wells, as illustrated in Fig. 14.

More active strategies to increase capillary trapping include co-injection of CO_2 and brine, the injection of chase brine after injection (Juanes et al., 2006; Qi et al., 2009) and recycling produced brine (Cameron and Durlofsky, 2012). In this case, capillary

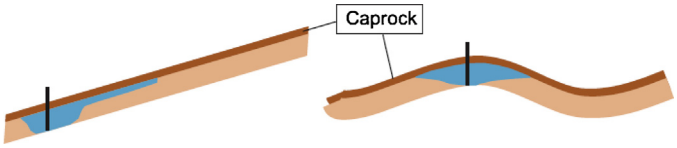

Fig. 13. A schematic of storage in open aquifers. The injection well is shown as the vertical black line. On the left, CO_2 can migrate upwards beneath the caprock, but the aquifer itself is not closed. However, if capillary trapping leaves a trail of ganglia, the movement of the is significantly impeded and long-term storage is possible. The right figure shows trapping under a dome-shaped caprock – even here, however, migration laterally is possible after further injection. Figure taken from Goater et al. (2013).

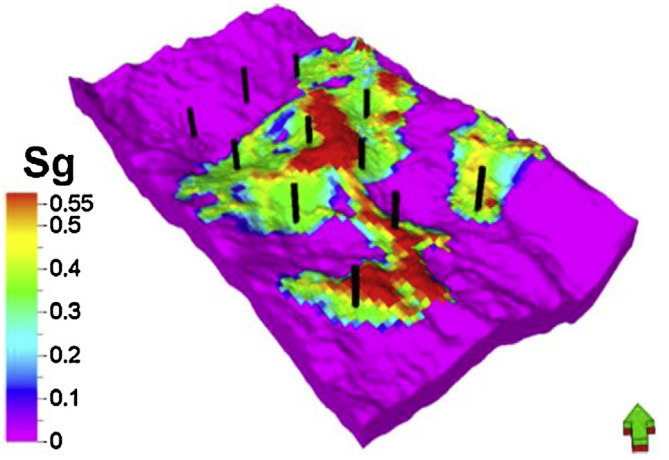

Fig. 14. The results of a numerical simulation of 10,000 years of CO_2 migration in an open aquifer under the North Sea: the extent of the domain shown is around 40 km with a natural groundwater flow in the direction of the arrow. Carbon dioxide is trapped under local traps in the top surface of the aquifer and – more extensively – by capillary trapping as it migrates, slowly, upwards. The injection wells are shown by the black lines and the CO_2 saturation on the top surface of the aquifer is shown. Figure from Goater et al. (2013).

trapping is artificially enhanced, as water is injected deliberately into the formation to trap CO_2. The injected brine, since it traps a significant fraction of the CO_2, moves rapidly through the formation, rendering most of the CO_2 immobile in a few years after injection. Furthermore, co-injection decreases the apparent viscosity and density contrast between the injected fluids and the resident brine, allowing the CO_2 to be displaced into more of the aquifer, and hence increasing storage capacity.

It is possible to design a process that – for typical storage conditions – would have 90% of the capillary trapped with only a few years of chase brine injection while increasing storage capacity. The major cost penalty comes from the injection of water: the mass required is around 25% of the mass of injected CO_2 (Qi et al., 2009).

From an environmental perspective, injection and subsequent migration is often viewed as a passive process, with storage capacity and security governed by unstoppable natural processes. However, from an engineering perspective, well placement, injection rates and monitoring are part of an active process where we design injection to maximize capacity and security. In particular, brine injection can be considered one way to force CO_2 through more of the aquifer - rather than collecting at the top – and/or to render the CO_2 rapidly immobile.

4.4. Field scale observations of residual trapping

Direct observations of residual trapping in the reservoir are currently limited to those technologies that can be applied in well bores. Tomographic techniques that can image the entire plume, e.g., surface based seismic surveys, cannot currently be used to

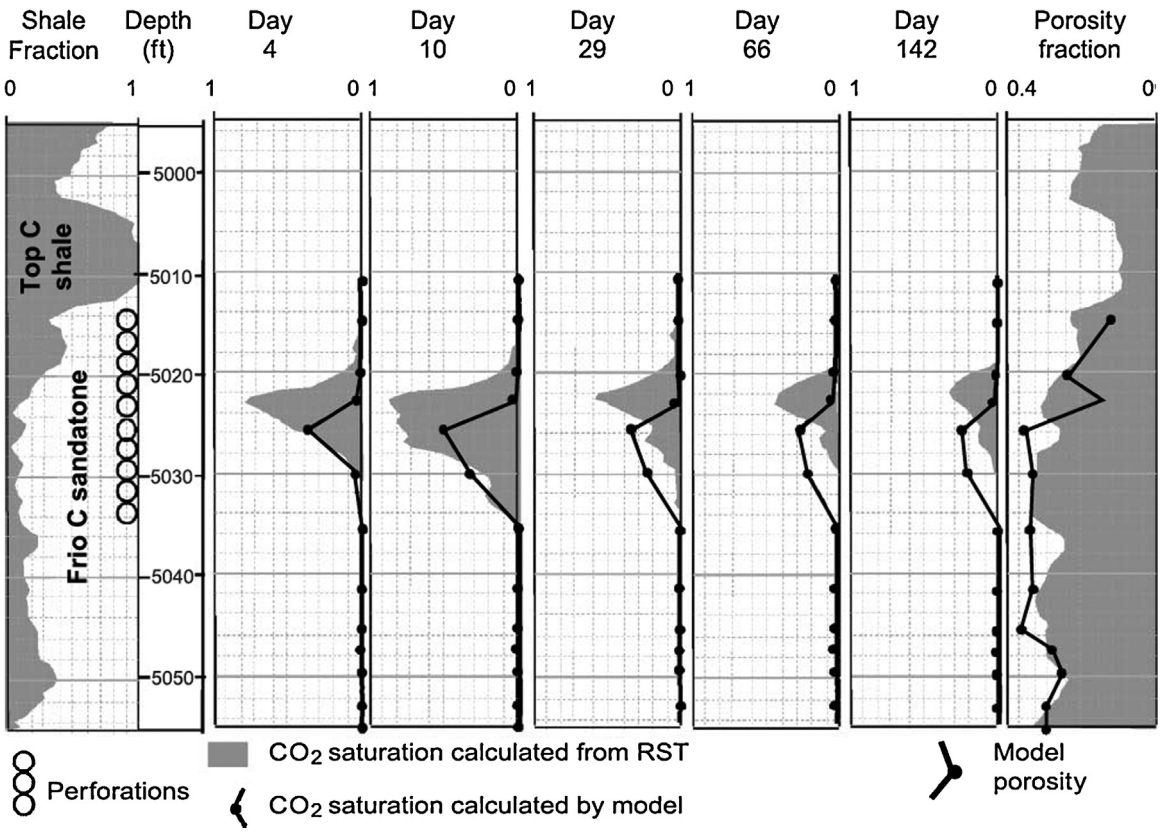

Fig. 15. Near well-bore CO_2 saturation measured in an observation well of the Frio pilot CO_2 storage experiment as a small CO_2 plume migrated updip past the well. Injection ceased after 10 days and saturations measured on days 29, 66 and 142 were constant within the uncertainty of the measurement, suggesting the persistence of residually trapped CO_2. Figure from Hovorka et al. (2006).

estimate CO_2 saturation, and by extension, residually trapped CO_2. It is expected that in industrial scale projects measurements in wells that provide observations of saturation at specific locations, combined with seismic surveys that detail the spatial extent of the CO_2 plume, and numerical simulation will be used in combination to estimate the total amount of residually trapped CO_2 (Doughty et al., 2008). This approach has been demonstrated at two pilot CO_2 injection experiments, the Frio site in Eastern Texas (Hovorka et al., 2006; Sakurai et al., 2006; Müller et al., 2007; Doughty et al., 2008) and the Nagaoka site in Japan (Xue et al., 2006; Saito et al., 2006; Mito and Xue, 2011).

The Frio project is summarised by Hovorka et al. (2006) and further details of the saturation observations can be found in Sakurai et al. (2006) and Müller et al. (2007). Sixteen hundred tons of CO_2 were injected into a permeable (1–2.5 Darcy) sandstone 1500 m deep over 10 days and allowed to migrate up along a steeply dipping (18°) confining shale layer. Near-well observations were made using Schlumberger's pulse neutron logging reservoir saturation tool in the injection well and an observation well 30 m up dip from the injection site.

Saturations observed from the observation well are shown in Fig. 15. They showed the arrival and growth of the plume over 10 days of injection followed by a decrease in saturation and ultimate stabilisation as the plume migrated buoyantly. In the observation well, CO_2 saturation peaked between 80 and 90% followed by a stabilisation at between 40 and 50%, a degree of trapping that corresponded to a Land constant of $C \approx 1$ (see Section 3.2). The observations were also supported through cross-well seismic tomography that provided a qualitative image of the plume that corresponded well to the saturation profiles in the injection and observation wells.

A larger scale injection was performed near the city of Nagaoka in the Niigata prefecture in Japan (Xue et al., 2006; Saito et al., 2006; Sato et al., 2011; Mito and Xue, 2011). Here ten thousand tons of CO_2 were injected over 18 months into a steeply dipping (15°) 7 millidarcy sandstone formation 1100 m in the subsurface. Sonic, resistivity and neutron logging tools were deployed for monitoring in three observations wells, one 40 m down-dip from the injection site and two up-dip 60m and 120 m respectively. The logs were taken frequently during the injection (26 over an 18 month period) and continued with 11 further logs taken over 36 months following the end of injection (Sato et al., 2011; Mito and Xue, 2011). The CO_2 was only observed in the down-dip well and one of the up-dip wells. In the down-dip well, CO_2 saturation peaked 22 months after injection ceased at 60% and stabilised about 6 months later at around 30% saturation. In the well 60m updip from the injection site, CO_2 saturation peaked at 60% between 9 and 15 months after injection ceased and stabilised 21 months after injection also at around 30% CO_2 saturation. The large volumes and timescales involved provided a confirmation of the stability of residual trapping in the field.

Well testing can also serve as an important site characterisation tool to determine the residual trapping capacity at scales much larger than is possible from laboratory observations (Paterson et al., 2011; Zhang et al., 2011; Martinez-Landa et al., 2013; Rasmusson et al., 2014). Extensive development and testing of an injection test and a number of techniques for observing the residually trapped CO_2 have been deployed as a part of the CO2CRC pilot Otway project in South Eastern Australia (Paterson et al., 2011; Zhang et al., 2011; LaForce et al., 2014; Myers et al., 2014). A detailed summary of the test design and preliminary results are provided in Paterson et al. (2011). A single injection and fluid withdrawal sequence was used

simultaneous with five observation techniques: history matching injection and production pressure time-series, the neutron logging tool used in the Frio and Nagaoka test sites for observations near the wellbore, thermal logging, the use of non-reactive partitioning tracers, the use of a reactive tracer and a dissolution test. The history matching, near well bore pulse-neutron logging and partitioning tracer tests estimated average residual saturations of 15–20% and were consistent with each other while complications in the injection sequence compromised the observations made for the reactive tracer test. An analysis in Zhang et al. (2011) also showed that confidence in the overall characterisation was significantly increased through the deployment of several simultaneous interpretation techniques.

5. Key outstanding questions: reservoir heterogeneity and mixed-wet systems

There are many outstanding uncertainties around all aspects of capillary trapping and it remains an area of active research. We highlight two here – the impact of reservoir heterogeneity on trapping and capillary trapping in depleted hydrocarbon reservoirs with altered wettability – where insights from future research are likely to have a significant impact on reservoir characterisation and management for CO_2 storage.

5.1. Trapping and natural reservoir heterogeneity

A number of theoretical, numerical and experimental observations have begun to demonstrate the importance of natural rock heterogeneity at all scales on CO_2 trapped by capillary forces. Among the earliest modelling studies to identify capillary trapping as important, the works of Doughty and Pruess (2004) and Doughty (2007), were focused on the impacts of reservoir heterogeneity, represented by permeability heterogeneity, and demonstrated that there was a complex interplay between reservoir heterogeneity, flow property hysteresis and residual trapping. Ignoring any of these effects in the simulation led to significant changes in plume behaviour. Theoretical studies have been limited to consideration of distributions of locally impermeable clay lenses in permeable reservoirs (Hesse and Woods, 2010), but also show how reservoir heterogeneity can have an impact on plume sweep and thus residual trapping.

Saadatpoor et al. (2009) and more recently Meckel et al. (2015) showed how heterogeneity in the capillary pressure characteristic curves could lead to a kind of trapping by capillary forces that is much greater than would be estimated using the *IR* relationship and ignoring capillary heterogeneity. An experimental investigation reported in Krevor et al. (2011) also demonstrated saturation buildup and immobilisation due to capillary heterogeneities in an otherwise permeable sandstone.

These investigations have not yet resulted in a general framework for reservoir characterisation and incorporation of the impact of heterogeneity into modelling. Advances in this area will significantly increase the effectiveness of reservoir management for CO_2 storage.

5.2. Trapping and hysteresis in mixed-wet systems

While the observations for sandstones show water-wet behaviour it is known that organic rich material such as coal and surfaces that have been contaminated with hydrocarbons can exhibit mixed- or CO_2-wet behaviour (Iglauer et al., 2014a). It is therefore of interest to discuss the multiphase flow behaviour of such systems.

Numerous studies have investigated the impact of wettability on relative permeability and capillary pressure (as summarised by Anderson, 1987a,b), primarily in the context of hydrocarbon recovery. It is known that in oil-wet systems the maximum aqueous phase relative permeability can exceed that observed in water-wet systems; and that significant saturation change occurs at negative capillary pressures (that is the pressure in the aqueous phase exceeds the pressure in the non-aqueous phase). The impact of wettability upon the *IR* relationship – for both hydrocarbon and groundwater applications – is less well characterised. Few direct observations have been made of the effect of wettability alteration.

The work of Salathiel (1973) showed that oil saturations continued to decrease with water flooding in mixed wet systems up to 20 pore volumes of water injected. Expanding on this work Tanino and Blunt (2013) showed that oil saturation continued to decrease with over 100 pore volumes of water injected. The results of pore-scale simulation studies showed that when the residual was finally achieved, the relationship with initial saturation is complex, with the *IR* curve becoming convex with the maximum residual saturation occurring at an initial saturation below the maximum (Spiteri et al., 2008).

Carbon dioxide injection into depleted oil and gas fields represents a low-cost opportunity for CO_2 storage for many reasons including revenue from enhanced oil recovery and the ability to take advantage of existing reservoir characterisation and site infrastructure. Understanding migration and trapping for CO_2 in these systems should be a high priority for research.

6. Conclusion

In the ten years since the IPCC Special Report on Carbon Dioxide Capture and Storage (2005) a large body of theoretical, numerical and experimental research has led to a greatly increased understanding of capillary trapping during CO_2 storage. These studies have investigated areas ranging from the underlying physical processes at the pore scale to the effects of trapping on field scale fluid flow, storage security and sequestration capacity.

At the pore scale, capillary trapped ganglia of supercritical CO_2 have been observed in situ at reservoir conditions in several sandstone and carbonate rocks at reservoir conditions. Direct observations of in situ contact angles and ganglia size distributions have confirmed that CO_2 acts as a non-wetting phase in sandstones and carbonate rocks.

At the rock core scale a significant number of characteristic *IR* curves and large body of individual initial-residual saturation point pairs are now available in the public literature for a range of sandstone and carbonate rock types and reservoir conditions. They show that residual trapping will be significant, with trapped saturations at least 10% and more typically 30% of the pore volume of the rock, stable against subsequent displacement by brine and characteristic of water-wet systems, consistent with the observations made at the pore scale. The observations demonstrate that it is difficult to predict in advance the *IR* relationship for a rock in the absence of a measurement. They do provide some indication of the range of possible values with the Land model bounding data with constants between the values $0.2 < C < 5$.

Theoretical and numerical models have shown that residual trapping and relative permeability hysteresis have a first order impact on the movement of a plume, with greater capillarity and hysteresis resulting in more capillary trapping, and capillary trapping itself resulting in significant reductions in the rate and extent of plume migration. This has led numerous national storage capacity assessments to incorporate the affects of capillary trapping in the modelling for their assessment, resulting in as much as 95% of the storage capacity attributable to the capacity for residual trapping.

Engineering strategies have also developed to maximise residual trapping. They make use of well placement, injection man-

agement and circulation of brine to enhance the rates and amount of residual trapping through enhancements in plume migration, sweep and imbibition.

Field scale observations of residual trapping have confirmed the formation and stability of thousands of tons of residually trapped CO_2 from a buoyantly migrating plume for up to timescales of years. Additionally, several single-well field tests have been deployed demonstrating their utility in site characterisation for residual trapping.

Key outstanding uncertainties that will likely have further impact on reservoir characterisation and management include the characterisation of the impact of reservoir rock heterogeneity on capillary trapping, and the character of capillary trapping in depleted oil reservoirs with altered wettability.

Overall, a clear picture has emerged of the importance of capillary trapping in CO_2 storage. It is a process that can be well constrained by laboratory and field scale observations and effectively modelled by theoretical models and detailed numerical simulation. Capillary trapping plays a key role in storage security, slowing plume migration, increasing storage capacity, and enhancing reservoir integrity.

Acknowledgements

Sam Krevor, Martin Blunt, Catriona Reynolds, Ali Al-Menhali and Ben Niu would like to acknowledge funding assistance from the Qatar Carbonates and Carbon Storage Research Centre provided jointly by Qatar Petroleum, Shell, and the Qatar Science & Technology Park.

The authors wish to thank two anonymous reviewers for their valuable comments on an initial draft of this review.

References

Akbarabadi, M., Piri, M., 2013. Relative permeability hysteresis and permanent capillary trapping characteristics of supercritical CO_2/brine systems: an experimental study at reservoir conditions. Adv. Water Resour. 52, 190–206.

Akbarabadi, M., Piri, M., 2015. Co-sequestration of SO_2 with supercritical CO_2 in carbonates: an experimental study of capillary trapping, relative permeability, and capillary pressure. Adv. Water Resour. 77, 44–56.

Al-Menhali, A., Krevor, S., 2013. Pressure, temperature and ionic strength effects on the wettability of CO_2-brine-sandstone system: Core-scale contact angle measurements. In: International Symposium of the Society of Core Analysts held in Napa Valley, California, 16-19 September, SCA2013-003.

Anderson, W., 1987a. Wettability literature survey – Part 4: Effects of wettability on capillary pressure. J. Petrol. Technol. 39, 1283–1300.

Anderson, W., 1987b. Wettability literature survey. Part 5: The effects of wettability on relative permeability. J. Petrol. Technol. 39, 1453–1468.

Andrew, M., Bijeljic, B., Blunt, M., 2013. Pore-scale imaging of geological carbon dioxide storage under in situ conditions. Geophys. Res. Lett. 40, 3915–3918.

Andrew, M., Bijeljic, B., Blunt, M., 2014a. Pore-scale contact angle measurements at reservoir conditions using X-ray microtomography. Adv. Water Resour. 68, 24–31.

Andrew, M., Bijeljic, B., Blunt, M.J., 2014b. Pore-scale imaging of trapped supercritical carbon dioxide in sandstones and carbonates. Int. J. Greenh. Gas Control 22, 1–14.

Armstrong, R., Berg, S., 2013. Interfacial velocities and capillary pressure gradients during Haines jumps. Phys. Rev. E 88, 043010.

Armstrong, R., Porter, M., Wildenschild, D., 2012. Linking pore-scale interfacial curvature to column scale capillary pressure. Adv. Water Resour. 46, 55–62.

Bachu, S., 2013. Drainage and imbibition CO_2/brine relative permeability curves at in situ conditions for sandstone formations in Western Canada. Energy Proc. – 11th Int. Conf. Greenh. Gas Control Technol. 37, 4428–4436.

Bachu, S., 2015. Review of CO_2 storage efficiency in deep saline aquifers. Int. J. Greenh. Gas Control, http://dx.doi.org/10.1016/j.ijggc.2015.01.007 (in press).

Bandara, U., Tartakovsky, A., Palmer, B., 2011. Pore-scale study of capillary trapping mechanisms during CO_2 injection in geological formations. Int. J. Greenh. Gas Control 5, 1566–1577.

Bennion, D.B., Bachu, S., 2008. Drainage and imbibition relative permeability relationships for supercritical CO_2/brine and H_2S/brine systems in intergranular sandstone, carbonate, shale, and anhydrite rocks. SPE Reserv. Eval. Eng. 11, 487–496.

Bennion, D.B., Bachu, S., 2010. Drainage and imbibition CO_2/brine relative permeability curves at reservoir conditions for carbonate formations. In: SPE Annual Technical Conference and Exhibition, 19–22 September 2010, Florence, Italy, SPE 134028.

Benson, S., Cook, P., Anderson, J., Bachu, S., Nimir, H., Basu, B., Bradshaw, J., Deguchi, G., Gale, J., von Goerne, G., Heidug, W., Holloway, S., Kamal, R., Keith, D., Lloyd, P., Rocha, P., Senior, B., Thompson, J., Torp, T., WIldenborg, T., Wilson, M., Zarlenga, F., Zhou, D., Celia, M., Gunter, B., King, J.E., Lindegerg, E., Lombardi, S., Oldenburg, C., Pruess, K., Rigg, A., Stevens, S., WIlson, E., Whittaker, S., 2005. IPCC Special Report on Carbon Dioxide Capture and Storage. Chapter 5 – Underground Geologic Storage. Cambridge University Press.

Benson, S.M., Bennaceur, K., Cook, P., Davison, J., de Coninck, H., Farhat, K., Ramirez, A., Simbeck, D., Surles, T., Verma, P., Wright, I., 2012. Global Energy Assessment. Chapter 13. Carbon Capture and Storage. Cambridge University Press.

Berg, S., Ott, H., Klapp, S., Schwing, A., Neiteler, R., Brussee, N., Makurat, A., Leu, L., Enzmann, F., Schwarz, J., Kersten, M., Irvine, S., Stampanoni, M., 2013. Real-time 3d imaging of haines jumps in porous media flow. Proc. Natl. Acad. Sci. U. S. A. 110, 3755–3759.

Bikkina, P., 2011. Contact angle measurements of CO_2-water-quartz/calcite systems in the perspective of carbon sequestration. Int. J. Greenh. Gas Control 5, 1259–1271.

Blunt, M., Bijeljic, B., Dong, H., Gharbi, O., Iglauer, S., Mostaghimi, P., Paluszny, A., Pentland, C., 2013. Pore-scale imaging and modelling. Adv. Water Resour. 51, 197–216.

Blunt, M.J., Scher, H., 1995. Pore level modeling of wetting. Phys. Rev. E 52, 6387–6403.

Broseta, D., Tonnet, N., Shah, V., 2012. Are rocks still water-wet in the presence of dense CO_2 or H_2S? Geofluids 12, 280–294.

Burnside, N., Naylor, M., 2014. Review and implications of relative permeability of CO_2/brine systems and residual trapping of CO_2. Int. J. Greenh. Gas Control 23, 1–11.

Cameron, D.A., Durlofsky, L.J., 2012. Optimization of well placement, CO_2 injection rates, and brine cycling for geological carbon sequestration. Int. J. Greenh. Gas Control 10, 100–112.

Chalbaud, C., M.Robina, J.-M.L., Martina, F., Egermanna, P., Bertinb, H., 2009. Interfacial tension measurements and wettability evaluation for geological CO_2 storage. Adv. Water Resour. 32, 98–109.

Chaudhary, K., Cardenas, M.B., Wolfe, W.W., Maisano, J.A., Ketcham, R.A., Bennett, P.C., 2013. Pore-scale trapping of supercritical CO_2 and the role of grain wettability and shape. Geophys. Res. Lett. 40, 3878–3882.

Chiquet, P., Broseta, D., Thibeau, S., 2007. Wettability alteration of caprock minerals by carbon dioxide. Geofluids 7, 112–122.

Class, H., Ebigbo, A., Helmig, R., Dahle, H.K., Nordbotten, J.M., Celia, M.A., Audigane, P., Darcis, M., Ennis-King, J., Fan, Y., Flemisch, B., Gasda, S.E., Jin, M., Krug, S., Labregere, D., Beni, A.N., Pawar, R.J., Sbai, A., Thomas, S.G., Trenty, L., Wei, L., 2009. A benchmark study on problems related to CO_2 storage in geologic formations. Comput. Geosci. 13, 409–434.

Coles, M., Hazlett, R., Spanne, P., Soll, W., Muegge, E., Jones, K., 1998. Pore level imaging of fluid transport using synchrotron X-ray microtomography. J. Petrol. Sci. Eng. 19, 55–63.

Dias, M., Wilkinson, D., 1986. Percolation with trapping. J. Phys. A: Math. Gen. 19, 3131–3146.

Doughty, C., 2007. Modeling geologic storage of carbon dioxide: comparison of non-hysteretic and hysteretic characteristic curves. Energy Convers. Manage. 48, 1768–1781.

Doughty, C., Freifeld, B.M., Trautz, R.C., 2008. Site characterization for CO_2 geologic storage and vice versa: the Frio brine pilot, Texas, USA as a case study. Environ. Geol. 54, 1635–1656.

Doughty, C., Pruess, K., 2004. Modeling supercritical carbon dioxide injection in heterogeneous porous media. Vadose Zone J. 3, 837–847.

Dullien, F., 1992. Porous Media Fluid Transport and Pore Structure. Academic Press, Inc.

Eigestad, G.T., Dahle, H.K., Hellevang, B., Riis, F., Johansen, W.T., Oian, E., 2009. Geological modeling and simulation of CO_2 injection in the Johansen formation. Comput. Geosci. 13, 435–450.

El-Maghraby, R.M., Blunt, M.J., 2012. Residual CO_2 trapping in Indiana limestone. Environ. Sci. Technol. 47, 227–233.

Espinoza, D.N., Santamarina, J.C., 2010. Water-CO_2-mineral systems: Interfacial tension, contact angle, and diffusion–implications to CO_2 geological storage. Water Resour. Res. 46, W07537.

Farcas, A., Woods, A.W., 2009. The effect of drainage on the capillary retention of CO_2 in a layered permeable rock. J. Fluid Mech. 618, 349–359.

Farokhpoor, R., Bjorkvik, B., Lindeberg, E., Torsaeter, O., 2013. Wettability behaviour of CO_2 at storage conditions. Int. J. Greenh. Gas Control 12, 18–25.

Flannery, B., Deckman, H., Roberge, W., D'Amico, K., 1987. Three-dimensional X-ray microtomography. Science 237, 1439–1444.

Flett, M., Gurton, R., Taggart, I., 2004. The function of gas-water relative peremeability hysteresis in the sequestration of carbon dioxide in saline formations. In: SPE Asia Pacific Oil and Gas Conference and Exhibition, SPE-8845-MS.

Foster, W., 1973. A low-tension waterflooding process. J. Petrol. Technol. 25, 205–210.

Gammer, D., Green, A., Holloway, S., Smith, G., 2011. The Energy Technologies Institute's UK CO_2 storage appraisal project. In: Paper SPE 148426 in Proceedings of the SPE Offshore Europe Oil and Gas Conference and Exhibition.

Gasda, S., Nordbotten, J., Celia, M., 2009. Vertical equilibrium with sub-scale analytical methods for geological CO_2 sequestration. Comput. Geosci. 13, 469–481.

Georgiadis, A., Berg, S., Makurat, A., Maitland, G., Ott, H., 2013. Pore-scale micro-computed-tomography imaging: nonwetting-phase cluster-size distribution during drainage and imbibition. Phys. Rev. E 88, 1–9.
Goater, A., Bijeljic, B., Blunt, M., 2013. Dipping open aquifers – the effect of top-surface topography and heterogeneity on CO_2 storage efficiency. Int. J. Greenh. Gas Control 17, 318–331.
Golding, M.J., Huppert, H.H., Neufeld, J.A., 2013. The effects of capillary forces on the axisymmetric propagation of two-phase, constant-flux gravity currents in porous media. Phys. Fluids, 25.
Golding, M.J., Neufeld, J.A., Hesse, M.A., Huppert, H.E., 2011. Two-phase gravity currents in porous media. J. Fluid Mech. 678, 248–270.
Gupta, S.P., Trushenski, S.P., 1979. Micellar flooding – compositional effects on oil displacement. SPE Journal 19, 116–128.
Halland, E.K., Gjeldvik, I.T., Johansen, W.T., Magnus, C., Meling, I.M., Pedersen, S., Riis, F., Solbakk, T., Tappel, I., 2011. CO_2 Storage Atlas Norwegian North Sea. In: Technical Report Norweigian Petroleum Directorate.
Hassler, G., Brunner, E., 1945. Measurement of capillary pressures in small core samples. Petrol. Trans. AIME 160, 114–123.
Hesse, M., Orr Jr., F.M., Tchelepi, H., 2008. Gravity currents with residual trapping. J. Fluid Mech. 611, 35–60.
Hesse, M., Woods, A., 2010. Buoyant dispersal of CO_2 during geological storage. Geophys. Res. Lett., 37.
Hildenbrand, A., Schlomer, S., Krooss, B., Littke, R., 2004. Gas breakthrough experiments on pelitic rocks: comparative study with N_2, CO_2 and CH_4. Geofluids 4, 61–80.
Hovorka, S.D., Benson, S.M., Doughty, C., Freifeld, B.M., Sakurai, S., Daley, T.M., Kharaka, Y.K., Holtz, M.H., Trautz, R.C., Nance, H.S., Myer, L.R., Knauss, K.G., 2006. Measuring permanence of CO_2 storage in saline formations: the Frio experiment. Environ. Geosci. 13, 105–121.
Huppert, H.E., Neufeld, J.A., 2014. The fluid mechanics of carbon dioxide sequestration. Ann. Rev. Fluid Mech. 46, 255–272.
Iglauer, S., Paluszny, A., Pentland, C.H., Blunt, M.J., 2011. Residual CO_2 imaged with X-ray micro-tomography. Geophys. Res. Lett. 38, 21, L21403.
Iglauer, S., Pentland, C., Bush, A., 2014a. CO_2 wettability of seal and reservoir rocks and the implications for carbon geosequestration. Water Resour. Res., http://dx.doi.org/10.1002/2014WR015553 (in press).
Iglauer, S., Salamah, A., Sarmadivaleh, M., Liu, K., Phan, C., 2014b. Contamination of silica surfaces: Impact on water-CO_2-quartz and glass contact angle measurements. Int. J. Greenh. Gas Control 22, 325–328.
IPCC, 2005. IPCC Special Report on Carbon Dioxide Capture and Storage, Prepared by Working Group III of the Intergovernmental Panel on Climate Change. Cambridge University Press, Cambridge, United Kingdom/New York, NY, USA.
Jerauld, G., 1997. Prudhoe Bay gas/oil relative permeability. SPE Reserv. Eng. 12, 66–73.
Jerauld, G., Salter, S., 1990. Effect of pore-structure on hysteresis in relative permeability and capillary pressure: pore-level modelling. Transp. Porous Media 5, 103–151.
Joekar-Niasar, V., Doster, F., Armstrong, R., Wildenschild, D., Celia, M., 2013. Trapping and hysteresis in two-phase flow in porous media: a pore-network study. Water Resour. Res. 49, 4244–4256.
Juanes, R., MacMinn, C.W., Szulczewski, M.L., 2010. The footprint of the CO_2 plume during carbon dioxide storage in saline aquifers: storage efficiency for capillary trapping at the basin scale. Transp. Porous Media 82, 19–30.
Juanes, R., Spiteri, E., Orr Jr., F.M., Blunt, M., 2006. Impact of relative permeability hysteresis on geological CO_2 storage. Water Resour. Res. 42, W12418.
Jung, J.-W., Wan, J., 2012. Supercritical CO_2 and ionic strength effects on wettability of silica surfaces: Equilibrium contact angle measurements. Energy Fuels 26, 6053–6059.
Karpyn, Z., Piri, M., Singh, G., 2010. Experimental investigation of trapped oil clusters in a water-wet bead pack using X-ray microtomography. Water Resour. Res. 46, W04510.
Killough, J., 1976. Reservoir simulation with history-dependent saturation functions. SPE J. 16, 37–48.
King, J.E., Paterson, L., 2002. Engineering aspects of geological sequestration of carbon dioxide. In: Asia Pacific Oil and Gas Conference and Exhibition, SPE 77809.
Kleppe, J., Delaplace, P., Lenormand, R., Hamon, G., Chaput, E., 1997. Representation of capillary pressure hysteresis in reservoir simulation. In: SPE Annual Technical Conference and Exhibition, 5–8 October, San Antonio, TX, SPE 38899.
Krevor, S.C.M., Pini, R., Li, B., Benson, S.M., 2011. Capillary heterogeneity trapping of CO_2 in a sandstone rock at reservoir conditions. Geophys. Res. Lett. 38, L15401.
Krevor, S.C.M., Pini, R., Zuo, L., Benson, S.M., 2012. Relative permeability and trapping of CO_2 and water in sandstone rocks at reservoir conditions. Water Resour. Res. 48, W02532.
Kumar, A., Ozah, R., Noh, M., Pope, G., Bryant, S., Sepehmoori, K., Lake, L., 2005. Reservoir simulation of CO_2 storage in deep saline aquifers. SPE J. 10, 336–348.
LaForce, T., Ennis-King, J., Boreham, C., Paterson, L., 2014. Residual CO_2 saturation estimate using noble gas tracers in a single-well field test: The CO2CRC Otway project. Int. J. Greenh. Gas Control 26, 9–21.
Lake, L., Johns, R., Rossen, B., Pope, G., 2014. Fundamentals of Enhanced Oil Recovery. Society of Petroleum Engineers, TX, USA.
Land, C.S., 1968. Calculation of imbibition relative permeability for two- and three-phase flow from rock properties. SPE J. 8, 149–156.
Larson, R., Davis, H., Scriven, L., 1981. Displacement of residual nonwetting fluid from porous media. Chem. Eng. Sci. 36, 75–85.
Lenhard, R., Parker, J., 1987. A model for hysteretic constitutive relations governing multiphase flow. Water Resour. Res. 23, 2197–2206.
Lenormand, R., Touboul, E., Zarcone, C., 1988. Numerical models and experiments on immiscible displacements in porous media. J. Fluid Mech. 189, 165–187.
Lenormand, R., Zarcone, C., Sarr, A., 1983. Mechanism of the displacement of one fluid by another in a network of capillary ducts. J. Fluid Mech. 135, 337–353.
Li, X., Akbarabadi, M., Karpyn, Z.T., Piri, M., Bazilevskaya, E., 2015. Experimental investigation of carbon dioxide trapping due to capillary retention in saline aquifers. Geofluids, http://dx.doi.org/10.1111/gfl.12127
Lu, J., Kordi, M., Hovorka, S.D., Meckel, T.A., Christopher, C.A., 2012. Reservoir characterisation and complications for trapping mechanisms at Cranfield CO_2 injection site. Int. J. Greenh. Gas Control.
Ma, T., Youngren, T., 1994. Performance of immiscible water-alternating-gas (IWAG) injection at Kuparuk River Unit. In: North Slope Alaska. SPE Annual Technical Conference and Exhibition, New Orleans, Louisiana.
MacMinn, C.W., Szulczewski, M., Juanes, R., 2011. CO_2 migration in saline aquifers. Part 2. Capillary and solubility trapping. J. Fluid Mech. 688, 321–351.
MacMinn, C.W., Szulczewski, M.L., Juanes, R., 2010. CO_2 migration in saline aquifers. Part 1. Capillary trapping under slope and groundwater flow. J. Fluid Mech. 662, 329–351.
Martinez-Landa, L., Rotting, T.S., Carrera, J., Russian, A., Dentz, M., Cubillo, B., 2013. Use of hydraulic tests to identify the residual CO_2 saturation at a geological storage site. Int. J. Greenh. Gas Control 19, 652–664.
Meckel, T.A., Bryant, S.L., Ganesh, P.R., 2015. Characterization and prediction of CO_2 saturation resulting from modelling buoyant fluid migration in 2D heterogeneous geologic fabrics. Int. J. Greenh. Gas Control 34, 85–96.
Mito, S., Xue, Z., 2011. Post-injection monitoring of stored CO_2 at the Nagaoka pilot site: 5 years time-lapse well logging results. Energy Proc. – 10th Int. Conf. Greenh. Gas Control Technol. 4, 3284–3289.
Mohanty, K., Davis, H., Scriven, L., 1987. Physics of oil entrapment in water-wet rock. SPE Reserv. Eng. 2, 113–128.
Morrow, N.R., 1990. Wettability and its effect on oil recovery. J. Petrol. Technol. 42 (12), 1476–1484.
Müller, N., Ramakrishnan, T.S., Boyd, A., Sakruai, S., 2007. Time-lapse carbon dioxide monitoring with pulsed neutron logging. Int. J. Greenh. Gas Control 1, 456–472.
Myers, M., Stalker, L., LaForce, T., Pejcic, B., Dyt, C., Ho, K.-B., Ennis-King, J., 2014. Field measurement of residual carbon dioxide saturation using reactive ester tracers. Chem. Geol., http://dx.doi.org/10.1016/j.chemgeo.2014.02.002 (in press).
Naar, J., Henderson, J., 1961. An imbibition model – its application to flow behavior and the prediction of oil recovery. SPE J. 1, 61–70.
Niu, B., Al-Menhali, A., Krevor, S.C., 2015. The impact of reservoir conditions on the residual trapping of carbon dioxide in Berea sandstone. In: Water Resour. Res., http://dx.doi.org/10.1002/2014WR016441 (in press).
Nordbotten, J., Dahle, H., 2011. Impact of the capillary fringe in vertically integrated models for CO_2 storage. Water Resour. Res. 47, W02537.
Øren, P., Bakke, S., Arntzen, O., 1998. Extending predictive capabilities to network models. SPE J. 3, 324–336.
Paterson, L., Boreham, C., Bunch, M., Ennis-King, J., Freifeld, B., Haese, R., Jenkins, C., Raab, M., Singh, R., Stalker, L., 2011. The CO2CRC Otway stage 2b residual saturation and dissolution test: test concept, implementation and data collected. In: Milestone Report to ANLEC.
Pentland, C.H., El-Maghraby, R.M., Iglauer, S., Blunt, M.J., 2014. The toroidal porous plate: a new method to facilitate waterflooding. In: International Symposium of the Society of Core Analysts, Avignon, France, 8–11 September, SCA2014-068.
Pentland, C.H., El-Maghraby, R., Iglauer, S., Blunt, M.J., 2011. Measurements of the capillary trapping of super-critical carbon dioxide in Berea sandstone. Geophys. Res. Lett. 38, L06401.
Pentland, C.H., Itsekiri, E., Mansoori, S.K.A., Iglauer, S., Bijeljic, B., Blunt, M.J., 2010. Measurement of nonwetting-phase trapping in sandpacks. SPE J. 15, 274–281.
Pini, R., Benson, S.M., 2013. Simultaneous determination of capillary pressure and relative permeability curves from core-flooding experiments with various fluid pairs. Water Resour. Res. 49, 3516–3530.
Plug, W., Bruining, J., 2007. Capillary pressure for the sand-CO_2-water system under various pressure conditions: application to CO_2 sequestration. Adv. Water Resour. 30, 2339–2353.
Pruess, K., Xu, T., Apps, J., Garcia, J., 2003. Numerical modeling of aquifer disposal of CO_2. SPE J. 8, 49–60.
Qi, R., LaForce, T., Blunt, M., 2009. Design of carbon dioxide storage in aquifers. Int. J. Greenh. Gas Control 3, 195–205.
Ransohoff, T., Radke, C., 1988. Laminar flow of a wetting fluid along the corners of a predominantly gas-occupied noncircular pore. J. Colloid Interface Sci. 121, 392–401.
Rasmusson, K., Rasmusson, M., Fagerlund, F., Bensabat, J., Tsang, Y., Niemi, A., 2014. Analysis of alternative push-pull-test-designs for determining in situ residual trapping of carbon dioxide. Int. J. Greenh. Gas Control 27, 155–168.
Reynolds, C.A., Blunt, M.J., Krevor, S.C., 2013. The impact of interfacial tension on multiphase flow in the CO_2-brine-sandstone system. Am. Geophys. Union Fall Meet., L1366.
Roof, J., 1970. Snap-off of oil droplets in water-wet pores. SPE J. 10, 85–91.
Ruprecht, C., Pini, R., Falta, R., Benson, S., Murdoch, L., 2014. Hysteretic trapping and relative permeability of CO_2 in sandstone at reservoir conditions. Int. J. Greenh. Gas Control 27, 15–27.
Saadatpoor, E., Bryant, S.L., Sepehrnoori, K., 2009. New trapping mechanism in carbon sequestration. Transp. Porous Media 82, 3–17.
Saito, H., Nobuoka, D., Azuma, H., Xue, Z., Tanase, D., 2006. Time-lapse crosswell seismic tomography for monitoring injected CO_2 in an onshore aquifer, Nagaoka, Japan. Explor. Geophys. 37, 30–36.

Sakurai, S., Ramakrishnan, T.S., Boyd, A., Müller, N., Hovorka, S.D., 2006. Monitoring saturation changes for CO_2 sequestration: Petrophysical support of the Frio brine pilot experiment. Petrophysics 47, 483–496.

Salathiel, R., 1973. Oil recovery by surface film drainage in mixed-wettability rocks. J. Petrol. Technol. 25, 1216–1224.

Saraji, S., Goual, L., Piri, M., Plancher, H., 2013. Wettability of supercritical carbon dioxide/water/quartz systems: Simultaneous measurement of contact angle and interfacial tension at reservoir conditions. Langmuir 29, 6856–6866.

Sato, K., Mito, S., adn Hiroshi Ohkuma, T.H., Saito, H., Watanabe, J., Yoshimura, T., 2011. Monitoring and simulation studies for assessing macro- and meso-scale migration of CO_2 sequestered in an onshore aquifer: Experiences from the Nagaoka pilot site, Japan. Int. J. Greenh. Gas Control 5, 125–137.

Shell, 2011. SCAL Report. UK Carbon Capture and Storage Demonstration Competition, UKCCS-KT-S7.19-Shell-002.

Shi, J-Q., Xue, Z., Durucan, S., 2011a. Supercritical CO_2 core flooding and imbibition in Berea sandstone – imaging and numerical simulation. Energy Proc. 4, 5001–5008.

Shi, J-Q., Xue, Z., Durucan, S., 2011b. Supercritical CO_2 core flooding and imbibition in Tako sandstone – influence of sub-core scale heterogeneity. Int. J. Greenh. Gas Control 5, 75–87.

Silin, D., Tomutsa, L., Benson, S.M., Patzek, T.W., 2011. Microtomography and pore-scale modeling of two-phase fluid distribution. Transp. Porous Media 86, 495–515.

Smith, M., Campbell, D., Mackay, E., Polson, D., 2011. CO_2 Aquifer Storage Site Evaluation and Monitoring. Heriot-Watt University, Edinburgh.

Spiteri, E.J., Juanes, R., Blunt, M.J., Orr Jr., F.M., 2008. A new model of trapping and relative permeability hysteresis for all wettability characteristics. SPE J. 13, 277–288.

Suekane, T., Nobuso, T., Hirai, S., Kiyota, M., 2008. Geological storage of carbon dioxide by residual gas and solubility trapping. Int. J. Greenh. Gas Control 2, 58–64.

Suekane, T., Zhou, N., Hosokawa, T., Matsumoto, T., 2009. Direct observations of trapped gas bubbles by capillarity in sandy porous media. Transp. Porous Media 82, 111–122.

Szulczewski, M.L., MacMinn, C.W., Herzog, H.J., Juanes, R., 2012. Lifetime of carbon capture and storage as a climate-change mitigation technology. In: Proc. Natl. Acad. Sci. U. S. A, pp. 5185–5189.

Taber, J., 1969. Dynamic and static forces required to remove a discontinuous oil phase from porous media containing both oil and water. SPE J. 9, 3–12.

Tanino, Y., Blunt, M.J., 2013. Laboratory investigation of capillary trapping under mixed-wet conditions. Water Resour. Res. 49 (7), 4311–4319.

Valvatne, P., Blunt, M., 2004. Predictive pore-scale modeling of two-phase flow in mixed wet media. Water Resour. Res. 40, W07406.

Wang, F., 1988. Effect of wettability alteration on water/oil relative permeability, dispersion, and flowable saturation in porous media. SPE Reserv. Eng. 3, 617–628.

Wang, S., Edwards, I., Clarens, A., 2013. Wettability phenomena at the CO_2-brine-mineral interface: Implications for geologic carbon sequestration. Environ. Sci. Technol. 47, 234–241.

Warwick, P.D., Blondes, M.S., Brennan, S.T., Buursink, M.L., Cahan, S.M., Coleman, J.L., Cook, T.A., Corum, M.D., Covault, J.A., Craddock, W.H., DeVera, C.A., Doolan, C.,II, R. M.D., Drew, L.J., East, J.A., Freeman, P.A., Garrity, C.P., Gooley, K.J., Gosai, M.A., Jahediesfanjani, H., Lohr, C.D., Mars, J.C., Merrill, M.D., Olea, R.A., Roberst-Ashby, T.L., Rouse, W.A., Schruben, P.G., Schuenemeyer, J.H., Slucher, E.R., Varela, B.A., Verma, M.K.,;1; 2013. National Assessment of Geologic Carbon Dioxide Storage Resources – Results. Circular 1386 U.S. Geological Survey.

Wesch, A., Dahmen, N., Ebert, K., Schon, J., 1997. Grenzflächenspannungen, tropfengrößen und kontaktwinkel im zweiphasensystem H_2O/CO_2 bei temperaturen von 298 bis 333 K und drücken bis 30 MPa. Chem. Ing. Tech. 69, 942–946.

Wildenschild, D., Sheppard, A., 2013. X-ray imaging and analysis techniques for quantifying pore-scale structure and processes in subsurface porous medium systems. Adv. Water Resour. 51, 217–246.

Wilkinson, D., Willemsen, J., 1983. Invasion percolation: a new form of percolation theory. J. Phys. A: Math. Gen. 16, 3365–3376.

Xue, Z., Tanase, D., Watanabe, J., 2006. Estimation of CO_2 saturation from time-lapse CO_2 well logging in an onshore aquifer, Nagaoka, Japan. Explor. Geophys. 37, 19–29.

Yang, D., Gu, Y., Tontiwachwuthikul, P., 2008. Wettability determination of the reservoir brine-reservoir rock system with dissolution of CO_2 at high pressures and elevated temperatures. Energy Fuels 22, 504–509.

Zhang, Y., Freifeld, B., Finsterle, S., Leahy, M., Ennis-King, J., Paterson, L., Dance, T., 2011. Single-well experimental design for studying residual trapping of supercritical carbon dioxide. Int. J. Greenh. Gas Control 5, 88–98.

Zuo, L., Benson, S.M., 2014. Process-dependent residual trapping of CO_2 in sandstone. Geophys. Res. Lett. 41, 2820–2826.